Size Structured Epidemic Models

by

Griselle Torres García

A Dissertation Presented in Partial Fulfillment
of the Requirements for the Degree
Doctor of Philosophy

Approved February 2012 by the
Graduate Supervisory Committee:

Carlos Castillo-Chavez, Co-Chair
Zhilan Feng, Co-Chair
Sunmi Lee

ARIZONA STATE UNIVERSITY

May 2012

ABSTRACT

There have been many studies on the dynamics of infectious diseases considering the age structure of the population. This study analyzes the dynamics when the population is stratified by size. This kind of models are useful in the spread of a disease in fisheries where size matters, for microorganism populations or even human diseases that are driven by weight. A simple size-structured SIR model is introduced for which a threshold condition, R_0, equilibria and stability are established in special cases. Hethcote's approach is used to derive, from first principles, a parallel ODE size-structure system involving n-size classes.The specific case of $n = 2$ is partially analyzed. Constant effort harvesting is added to this model with the purpose of exploring the role of controls and harvesting. Different harvesting policies are proposed and analyzed through simulations.

To my family, specially my boys Santiago and Sebastian and my husband

Emilio, for their support and love.

ACKNOWLEDGMENTS

Special thanks to my mentor and co-advisor Professor Carlos Castillo-Chavez and his family. His patience and dedication have made a big difference in my life. To Professor Zhilan Feng for accepting been part of my committee and for the comments made on my work. Also, for been an inspiration of what a woman with kids can accomplish in life personally and professionally. To Professor Sunmi Lee for joining this team and all the moral support. Thanks to my boys: Sebastian and Santiago for being my motivation and for their unconditional love. For sharing me with my job and passion for mathematics. They are truly the motor that moves me every day and forces me to do better. To my husband Emilio for pushing me to finish and do better in everything I do. For been there with me when I needed him the most. And finally, special thanks to my parents and sister. Thanks to my parents that have never give up on me and that gave me the values to continue going forward. To my sister, the first doctor in the family, for her example of passion and dedication to work.

TABLE OF CONTENTS

CHAPTER Page

CHAPTER Page

LIST OF TABLES

LIST OF FIGURES

CHAPTER 1

INTRODUCTION

This research focuses in the study of size-structured epidemic models dynamics and the role of harvesting in it. Size is an important variable to describe population dynamics for many species, such as microorganisms, fish, plants and humans. In plants the size affects the exposure that a plant has to the sunlight. Size is also important in human diseases because a bigger person has higher chances of contact with other individuals, but also because a heavier person can have higher susceptibility to diseases given that the body has to work harder to do the regular functions and therefore it may affect the immune defense system. For example, the Center for Disease Control and prevention (CDC) has obesity as primary risk factor for diabetes. The Diabetes Prevention Program, a federal study, showed that people at high risk for diabetes can delay or prevent the disease by losing a small amount of weight.

In fisheries it has been extensively studied that fish of different size have different susceptibilities to some diseases (Becker, Speare and Dohoo 2005 [2]; Perelberg, Smirnov, Hutoran, Diamant, Bejerano and Kolter 2003 [23]; Aranguren, Tafalla, Novoa and Figueras 2002 [1]; Bowser, Wooster and Earnest-Koons 1997 [3]; LaPatra, Groberg, Rohovec and Fryer 1990 [20]). Becker at. al. [2]studied the effect of feeding ratio and fish size on transmission of Loma salmonae in

salmonids. With survival analysis, which consists of using the time until first appearance of the disease as comparison measure, they analyzed their results. The experiment performed to determine the effect of fish size consisted of 300 salmonids placed in seven tanks, one control with no pathogen and two of each size class (small, medium and large). Significant differences were detected; small fish developed disease faster and as size increased disease susceptibility decreased.

Another experiment performed by Perelberg et.al. [23] in spring of 1998 when a new disease was causing high mortality on common carps in Israel showed that small young fish were more susceptible to the disease. In 2002, Aranguren at al. [1] studied the transmission of encephalopathy and retinopathy in sea beam. They observed that onset of the disease occurred earlier for smaller sea beams than bigger ones and mortality was higher for smaller fish. Bowser et. al. [3] in 1997, were also interested in the effects of fish age, specifically in the transmission of Wallaye Dermal Sarcoma in Wallayes. They injected tumor filtrates on fish for 25 weeks and observed more infections on 12-week old fish than in 1-year old fish. In all of these cases the environment is also affected by size, then it is assumed that vital rates such as mortality, fertility and growth rates are dependent on size. The size in fish also determines harvesting policies

because it is desired to catch big fish instead of very small ones. Then if there is higher susceptibility for smaller fish and harvesting is targeted towards bigger fish that leaves more infections in the areas. It is also alarming that harvested fish are usually replaced with small fish, which are more susceptible to the diseases. By common sense this explains how the usual harvesting policies may cause bigger outbreaks, and by implementing different strategies can eradicate a disease or lower endemic levels.

In this dissertation we will present the epidemiological applications of the size-structured model. We will use as motivation the studies on fish populations, as these populations are a great example of populations were size matters. And since the underlying motivator fish we will explore how harvesting (generalized size-specific predation) affects the dynamics of a disease. We will start with a model of partial differential equations for which we will perform analysis of non-uniform steady state distributions, basic reproductive number, and local stability in special cases. And by using a comparable model involving an arbitrary number of ordinary differential equations we will explore with simulations the effect of different harvesting strategies. Finally, we will study a control theory problem and we will compare the results with the ones obtained from the simulations of the ODE model under different parameter regimes.

This dissertation introduces a size-structured model for the dynamics of a fish population in Chapter 2. The disease-free stable size distribution and a unique endemic steady state distribution are identified. Further in Chapters 3, we introduce and analyze an SIR model that could be used to describe communicable diseases in, for example, fish populations. The basic reproductive numbers, infection-free steady distributions and endemic steady distributions are identified and conditions for local stability (infection-free case) are determined using exponential perturbations. In Chater 4, an ordinary differential equations model is derived from first principles and some simulations are performed to explore the effect of different harvesting strategies. Chapter 5 describes the study of harvesting in the size-structured model when the populations include sick individuals. In this work, we are considering constant effort harvesting which basically assumes that the harvesting rate depends on the number of individuals in the population. First, it is assumed that the harvesting rates are only dependent on size and not time. For this case numerical simulations are performed to determine the critical harvesting rate in order to control a disease. Time dependent harvesting is analyzed where a maximum and minimum are set with the aid of ”controls”. Two different harvesting strategies are used as methods of control of the disease for a population divided into just two-size groups. The first

strategy uses harvesting as control, but the elements of the population harvested are not replaced, therefore the harvesting keeps reducing the population as time goes on. In the second strategy, the individuals harvested are replaced with susceptible new comes of minimal size. The cases analyzed include low and high harvesting rates and combinations of low and high maximum harvesting rates.

CHAPTER 2

SIZE STRUCTURED EPIDEMIC MODEL

Population heterogeneity is a factor in the study of the population dynamics. Studies of many species in the past have considered age and size structure; Busenberg, S. et al. [6], Castillo-Chavez, C. [8], Castillo-Chavez et al. [4] [9], Hethcote, H.W. [13], Hoppensteadt, F. [14], Kato, N. [16], Kato, N. et al. [17], Nisbet, R.M. [22], Sanchez, D.A. [25] [26], Sinko, J.W. [27]. This dissertation studies the epidemiological applications of the size-structured models and introduces harvesting in this context. The first chapter makes on some observations on size-structured models in the presence and absence of harvesting in disease-free populations.

2.1. IBV problem for Size-Structured Population

This section starts from the Gurney-Nisbet one-sex population model [22] with per capita growth rate g, per capita fertility function f, and per capita death rate θ, all size-specific, i.e. dependent only on m. Furthermore,$\eta(t,m)$, the density of individuals is naturally dependent on size. Changes in the size distribution are assumed to be due to death and/or growth only. The resulting dynamics are

represented by the following initial boundary value problem (IBVP).

$$\frac{\partial \eta(t,m)}{\partial t} + g(m)\frac{\partial \eta(t,m)}{\partial m} = -\theta(m)\eta(t,m)$$

$$\eta(t,m_0) = \int_{m_0}^{\infty} f(m')\eta(t,m')dm'$$

$$\eta(0,m) = \eta_0(m) \tag{2.1}$$

where $\eta(t,m_0)$ represents new borns per unit of time with m_0 being the size at birth and $\eta(0,m)$ is the inital size density. The definitions of parameters and parameter functions are listed in Table 1. Model rates and functions description with units are as follows:

Symbol	Definition	Units
$g(m)$	growth function	size/(time · individual)
$f(m)$	fertility function	individuals/(time · individual)
$\theta(m)$	death rate	individuals/(time · individual)
$\eta(t,m)$	size density of individuals	individuals
$\eta(t,m_0)$	recruitment density	individuals

TABLE 1: Model Rates and Functions

This model is given by a linear homogeneous partial differential equation with initial conditions and boundary conditions that depend on the unknown density. Using well known results (see Castillo-Chavez, C. [9]) it is known that every solution $\eta(t,m)$ approaches a separable solution as time approaches infinity uniformly on compact sets. Hoppenstead [14] and Langlais et al [18] there

are theorems (including Tauberian theorems) that guarantee that all solutions for systems of the type (2.1) approach a separable solution as $t \to \infty$ are cited or noted. As Hoppenstead describes in [14], the proportion in any size "bracket" approaches a constant value as $t \to \infty$ and, it is in this sense that the size distribution of the population approaches the so called "stable size" distribution $[e^{qt}M(m)]$.

Theoretical results make it possible to explicitly identify the stable size distribution $[M(m)]$ through a search for separable solutions. If we let $\eta(t,m) = e^{qt}M(m)$ in (2.1) then the stable size distribution are determined as follows:

$$\begin{aligned} qe^{qt}M(m) + g(m)e^{qt}M'(m) &= -\theta(m)e^{qt}M(m) \\ g(m)M'(m) &= -\theta(m)M(m) - qM(m) \\ \frac{M'(m)}{M(m)} &= -\frac{\theta(m)+q}{g(m)} \\ \ln\frac{M(m)}{M(m_0)} &= -\int_{m_0}^{m}\frac{\theta(m')+q}{g(m')}dm' \\ M(m) &= M(m_0)e^{-\int_{m_0}^{m}\frac{\theta(m')+q}{g(m')}dm'}. \end{aligned} \tag{2.2}$$

The last expression for $M(m)$ is what we referred to as the stable-size distribution. The steady state size distribution is naturally an exponentially decaying function with decay factor ($\int_{m_0}^{m}\frac{\theta(m')+q}{g(m')}dm'$) since individuals get "heavier" or die (Castillo-Chavez [9]). The term $e^{-\int_{m_0}^{m}\frac{\theta(m')+q}{g(m')}dm'}$ represents the probability of

surviving from size m_0 to size m. Using the boundary condition in (2.1) we get

$$e^{qt}M(m_0) = \int_{m_0}^{\infty} f(m)e^{qt}M(m)dm$$

and the substitution of (2.2) leads to

$$M(m_0) = \int_{m_0}^{\infty} f(m)M(m_0)e^{-\int_{m_0}^{m}\frac{\theta(m')+q}{g(m')}dm'}dm.$$

Under the critical (obvious) assumption that $M(m_0) > 0$ we arrive at the following transcendental equation

$$1 = \int_{m_0}^{\infty} f(m)e^{-\int_{m_0}^{m}\frac{\theta(m')+q}{g(m')}dm'}dm =: F(q). \tag{2.3}$$

Equation (2.3) is the so-called Lotka characteristic equation, discovered by Lotka in 1922 in the context of age-structured populations. This equation allows us to define the population reproduction number as

$$\hat{R} = F(0) = \int_{m_0}^{\infty} f(m)e^{-\int_{m_0}^{m}\frac{\theta(m')}{g(m')}dm'}dm. \tag{2.4}$$

The function $F(q)$ has the propeties that $F'(q) = \Big(-\int_{m_0}^{m}\frac{1}{g(m')}dm'\Big)F(q) < 0$, $\lim_{q\to\infty}F(q) = 0$, for all $q \in (-\infty,\infty)$, and $F(0) = \hat{R}$. Thus, the equation (2.3) has a unique solution $q^* > 0$, i.e., $F(q^*) = 1$ if $F(0) > 1$ [$q^* < 0$ if $0 < F(0) < 1$]. Furthermore, the real solution q^* of the equation (2.3), is the unique dominant one in the sense that if $q = a + ib$ is a complex solution ($b \neq 0$) then $a \leq q$. In

order to verify the last statement, we let $H = \int_{m_0}^{m} \frac{b}{g(m')} dm'$ and observe that if $a+ib$ is a root then

$$\begin{aligned} 1 &= F(a+ib) = |F(a+ib)| \\ &= |\int_{m_0}^{\infty} f(m) e^{-\int_{m_0}^{m} \frac{\theta(m')+a+ib}{g(m')} dm'} dm| \\ &= |\int_{m_0}^{\infty} f(m) e^{-\int_{m_0}^{m} \frac{\theta(m')+a}{g(m')} dm'} [\cos(H) - i\sin(H)] dm| \\ &\leq F(a)|\cos(H) - i\sin(H)| \\ &= F(a). \end{aligned} \tag{2.5}$$

It follows that $F(a) \geq F(q^*)$. Since $F'(q) < 0$, we have $a \leq q^*$

Thus, we have obtained the following result.

Result 1 *If $\hat{R} < 1$ then $q^* < 0$ and there is exponential decay in the population, whereas if $\hat{R} > 1$ then $q^* > 0$ and there is exponential growth. If $\hat{R} = F(0) = 1$ then $q = 0$, in which case the population remains constant for all t.*

If we compare these results with those for age-structured models, we observe that the only difference is the presence of a non-constant function $g(m)$. In fact, a change of variable would bring us back to the age-structured framework (see Castillo-Chavez [9]). However, here I decided to write it all up explicitly in terms of $g(m)$. Recall the definition of $g(m) = \frac{dm}{dt}$, thus $g(m)$ is a nonnegative function and represents the per capita change in size per unit time when the indi-

vidual has size m. In other words, how much the organism's growth rate depends of the size of the organism with the probability of surviving from size m' to size m is $e^{-\int_{m'}^{m} \frac{\theta(m')+q}{g(m')} dm'}$, with $m' \geq m_0$ and $m' \leq m$.

Vital and transmission rates are dependent on size as well. Since, for example smaller organisms may have less movement and therefore contacts possibly causing less or more infections. If these organisms grow slow, transmission will be lower (faster) than if they grew fast. If they move less then they may live in a place where mobility is reduced by population density or behavior. In the case of age structure the survival probability is only dependent on the death rate, which is a function of age. Depending on the rate at which organisms die, in the different age groups, determines the life expectancy. In the case of size structure, with the function g, it is not just how they die at different size groups, but how they get to those size groups. If organisms grow faster then they may be more prone to survive to maximal size and therefore it is a different picture than growing slow.

2.2. Size Structure with Harvesting

In the size-structured model with harvesting considered in this section, it is assumed that the harvesting rate is a linear function of the population and that

the harvesting effort is size-dependent as it was done in age-structured models by Sanchez [25]. This is a common assumption in fisheries where the number of fish caught per unit time is proportional to the effort expended in fishing. In our case, we consider the following size-structured model for a "fish" population in which the effort function, denoted by $H(m)$, depend on the size of the individuals

$$\begin{aligned} \frac{d\eta}{dt} + g(m)\frac{d\eta}{dm} &= -\theta(m)\eta - H(m)\eta \\ \eta(t,m_0) &= \int_{m_0}^{\infty} f(m')\eta(t,m')dm' \\ \eta(0,m) &= \eta_0(m). \end{aligned} \tag{2.6}$$

Many studies on the effect of harvesting in the population have been done using models without a size structure. Sanchez [25] [26] studied age-structured models and harvesting. Here I follow Sanchez in order to investigate how size-dependent harvesting may affect the structure of the population. This allows for a comparison of the stable size distributions of the system with and without harvesting.

To analyze the system (2.6), we first consider the equation in the absence of harvesting and solve it using the method of characteristics. In this case the characteristics are the lines $t = \int_{m_0}^{m} \frac{1}{g(x)}dx + c$ where c is a constant. We make the same assumptions on $g(m)$ as in Castillo-Chavez [9] that guarantee the existence of non-intersecting characteristics for all time.

For $t > \int_{m_0}^{m} \frac{1}{g(x)}dx$, the function $\eta(t,m)$ describes the number of survivors to size m of the individuals $\eta(0, t - \int_{m_0}^{m} \frac{1}{g(x)}dx)$ that were born at time $t - \int_{m_0}^{m} \frac{1}{g(x)}dx$. To find an expression for $\eta(t,m)$ in this case, let $k(m) = \eta(m,t) = \eta(m, \int_{m_0}^{m} \frac{1}{g(x)}dm + c)$. Then from

$$g(m)\frac{dk}{dm} = \eta_t + g(m)\eta_m, \text{ and } \eta_t + g(m)\eta_m = -\theta(m)\eta$$

we get

$$g(m)\frac{dk}{dm} = -\theta(m)k \text{ and } \frac{dk}{dm} = \frac{-\theta(m)}{g(m)}k,$$

from which we have

$$k(m) = k(m_0)\exp\left[-\int_{m_0}^{m} \frac{\theta(x)}{g(x)}dx\right]$$

and

$$\eta(m,t) = \eta\left(m_0, t - \int_{m_0}^{m} \frac{1}{g(x)}dx\right)\exp\left[-\int_{m_0}^{m} \frac{\theta(x)}{g(x)}dx\right]. \qquad (2.7)$$

Consider next the case when $t \leq \int_{m_0}^{m} \frac{1}{g(x)}dx$, $\eta(t,m)$ is the number of survivors to size m of the individuals $\eta_0(\int_{m_0}^{m} \frac{1}{g(x)}dx - t)$ who where of size $\int_{m_0}^{m} \frac{1}{g(x)}dx - t$ at time zero. Let again $k(t) = \eta(m,t)$ and let $\int_{m_0}^{m} \frac{1}{g(x)}dx = z(m)$. Then $t = z(m)$; and thus, $m = z^{-1}(t)$. Hence, $k(t) = \eta(m,t) = \eta(z^{-1}(t),t)$. Note

that

$$\begin{aligned} g(m)\frac{dk}{dt} &= g(m)\eta_m + \eta_t \\ \Longrightarrow \quad g(z^{-1}(t))\frac{dk}{dt} &= g(m)\eta_m + \eta_t \\ \Longrightarrow \quad g(z^{-1}(t))\frac{dk}{dt} &= -\theta(m)\eta \\ \Longrightarrow \quad g(z^{-1}(t))\frac{dk}{dt} &= -\theta(z^{-1}(t))k \end{aligned} \tag{2.8}$$

Thus,

$$\frac{dk}{dt} = \frac{-\theta(z^{-1}(t))}{g(z^{-1}(t))}k$$

from which

$$k(t) = k(0)\exp\left[-\int_0^t \frac{\theta(z^{-1}(x))}{g(z^{-1}(x))}dx\right]$$

and

$$\eta(m,t) = \eta(z^{-1}(z(m)-t),0)\exp\left[-\int_0^t \frac{\theta(z^{-1}(x))}{g(z^{-1}(x))}dx\right].$$

For the above derivation we have used the fact that $m = z^{-1}(-c)$ for $t = 0$ and that from $t = z(m) + c$ we have $-c = z(m) - t$. Thus $x = z^{-1}(z(m)-t)$ for $t = 0$.

Let $B(t) = \eta(t, m_0)$ denote the number of births at t. Then, the solution of (2.1) is given by

$$\eta(m,t) = \begin{cases} \eta_0(z^{-1}(z(m)-t)\exp\left[-\int_0^t \frac{\theta(z^{-1}(x))}{g(z^{-1}(x))}dx\right] & \text{if } \int_{m_0}^m \frac{1}{g(x)}dx \geq t \\ B\left(t - \int_{m_0}^m \frac{1}{g(x)}dx\right)\exp\left[-\int_{m_0}^m \frac{\theta(x)}{g(x)}dx\right] & \text{if } \int_{m_0}^m \frac{1}{g(x)}dx < t. \end{cases}$$

Note that θ and f are independent of t. Then, $B(t)$ satisfies the integral equation

$$B(t) = \int_t^\infty F_0(x,t)dx + \int_{m_0}^t B\Big(t - \int_{m_0}^x \frac{1}{g(\alpha)}d\alpha\Big)K(x)dx \tag{2.9}$$

where

$$\begin{aligned} F_0(t,m) &= f(m)\eta_0(z^{-1}(z(m)-t))\exp\left[-\int_0^t \frac{\theta(z^{-1}(x))}{g(z^{-1}(x))}dx\right], \\ K(m) &= f(m)\exp\left[-\int_{m_0}^m \frac{\theta(x)}{g(x)}dx\right]. \end{aligned} \tag{2.10}$$

The equation for $B(t)$ is the well-known renewal equation (see Hoppenstead [14]). Note that $\int_t^\infty F_0(m,t)dx$ is a function of t only, which we will denote by $\psi(t)$. Then, the renewal equation (2.9) can be written as

$$B(t) = \psi(t) + \int_{m_0}^t B\Big(t - \int_{m_0}^x \frac{1}{g(\alpha)}d\alpha\Big)K(x)dx. \tag{2.11}$$

If we consider solutions of the form $B(t) = B^* e^{pt}$ in (2.11). Note that $\psi(t) \to 0$ as $t \to \infty$. Then, we get

$$B^* = B^* \int_{m_0}^\infty \exp\left(-p\int_{m_0}^x \frac{1}{g(\alpha)}d\alpha\right)K(x)dx.$$

Thus if $B^* > 0$ then the lotka-characteristic equation becomes

$$1 = \int_{m_0}^\infty \exp\left(-p\int_{m_0}^\infty \frac{1}{g(\alpha)}d\alpha\right)K(x)dx$$

with the right hand side, a function of $p \in \mathbb{C}$, defined as $\tilde{K}(p)$.

We observe that $\tilde{K}(0)$ gives the reproduction ratio $\Re$,

$$\tilde{K}(0) = \int_{m_0}^{\infty} f(m) \exp\left[-\int_{m_0}^{m} \frac{\theta(\alpha)}{g(\alpha)} d\alpha \right] dm = \Re \tag{2.12}$$

Further $\tilde{K}'(p) < 0$ for all $p \in (-\infty, \infty)$ with $lim_{p\to\infty}\tilde{K}(p) = 0$. It follows (as it was done before) that the equation $\tilde{K}(p) = 1$ has a unique real solution p_0. Moreover, $p_0 > 0$ if $\Re > 1$, and $p_0 < 0$ if $\Re < 1$. Similarly it can be shown that p_0 is the dominant root. That is, all other roots of this transcendental equation will have the real part less than p_0. Therefore, in the absence of harvesting, the population tends to a stable size distribution and in fact every solution approaches a separable solution

$$\eta(t,m) \Longrightarrow e^{p_0 t} B_0 \exp\left(-\int_{m_0}^{m} \frac{\theta(m') + p_0}{g(m')} dm' \right), \text{ as } t \to \infty, \tag{2.13}$$

in compact sets (Hoppensteadt [14]). Next, we consider the model with harvesting, i.e., $H(m) > 0$. The harvesting function is written as

$$H(m) = h\chi_{[c,\infty]}(m) \tag{2.14}$$

where h is a constant and

$$\chi_A(m) = \begin{cases} 1 & \text{if } x \in A \\ 0 & \text{otherwise.} \end{cases}$$

The solution of the model in this case is obviously formally the same as that without harvesting, except that the function $\theta(m)$ is now be replaced by $\theta(m) +$

$h\chi_{[c,\infty]}(m)$. The functions B, Φ and K are also replaced by B_1, Φ_1 and K_1, leading to the characteristic equation $K_1(p) = 1$ with

$$K_1(m) = f(m)\exp\left[-\int_{m_0}^{m} \frac{\theta(x) + h\chi_{[c,\infty]}(m)}{g(x)} dx\right]. \tag{2.15}$$

Therefore, it can be shown that there is a unique dominant real eigenvalue, denoted by p_c, such that $p_c < 0$ (> 0) if $R < 1$ (> 1). Thus, every size distribution approaches the separable solution

$$\eta(m,t) \to e^{p_c t} B_c \exp\left(-\int_{m_0}^{m} \frac{\theta(\alpha) + h\chi_{[c,\infty]}(\alpha) + p_c}{g(\alpha)} d\alpha\right), \text{ as } t \to \infty. \tag{2.16}$$

uniformly in compact sets. Here, $B_c = B_1(0)$ and thus the stable size distribution is determined from

$$B_c \exp\left(-\int_{m_0}^{m} \frac{\theta(\alpha) + h\chi_{[c,\infty]}(\alpha) + p_c}{g(\alpha)} d\alpha\right). \tag{2.17}$$

Following Hoppensteadt [14] , if we let

$$v(m,t) = \eta(m,t)\exp\left[p_c(t) + \int_{m_0}^{m} \frac{\theta(\alpha)}{g(\alpha)} - \frac{h\chi_{(c,\infty)}(\alpha)}{g(\alpha)} + \frac{p_c}{g(\alpha)} d\alpha\right] - B_c \tag{2.18}$$

we see that the function v satisfies

$$\begin{aligned} \frac{\partial v}{\partial t} + g(m)\frac{\partial v}{\partial m} &= 0, \\ v(m_0,t) &= \eta(m_0,t)e^{p_c t} - B_c. \end{aligned}$$

Given the definition of $\eta(m,t)$, $v(m_0,t) \to 0$ as $t \to \infty$ and $v(m,t)$ is constant along the characteristic lines, for any fixed $\hat{m} > 0$,

$$\max_{0\le m\le \hat{m}} \|v(m,t)\| \to 0 \text{ as } t \to \infty.$$

Given $\varepsilon > 0$, choose T so large that $\|v(m_0,t)\| < \varepsilon$ for $t \ge T$. Then $\|v(m,t)\| < \varepsilon$ in the entire triangular region $0 \le m \le t - T$ provided $t \ge T$. Therefore,

$$-e^{p_c t}\eta(m,t) \to B_c \exp\left(-\int_{m_0}^{m} \frac{\theta(\alpha) + h\chi_{[c,\infty]}(\alpha) + p_c}{g(\alpha)} d\alpha\right) \tag{2.19}$$

as $t \to \infty$,

If we compare the stable size distributions of the system without and with harvesting, we observe that the effect is reflected on p_0 and $h\chi_{[c,\infty]}(\alpha) + p_c$ in equations (2.13) and (2.16), respectively.

2.3. Conclusions

In this chapter, we re-introduce a size-structure model in the context of "fish" populations. We re-stated the corresponding work in Castillo-Chavez, C. [9], Sanchez [25], and Hoppensteadt [14] using an explicit representation of $g(m)$ in models with and without harvesting. For the model without harvesting we calculated the basic reproductive number and the stable size distribution. In the model with proportional harvesting, we also identified the limiting size distributions of the population are compared following the approach of Sanchez [25], [26]. This chapter sets up the theoretical framework where epidemiological models will be built, analyzed and explored in the next chapters.

CHAPTER 3

SIR MODEL

In the previous chapter we presented some observations of the partial differential equations system for size-structured model with and without harvesting. In this chapter we will describe and analyze the size-structured version of the SIR model and SI model that paralleled those developed using age-structure models [Hethcote, H.W. [13], Brauer, F. and Castillo-Chavez, C. [4]]. Later in Chapter 4 we will introduce an ordinary differential equations system for SIR and SI derived from first principles as well.

As in the classical SIR model, S denotes the susceptible individuals who are not infected but capable of contracting the disease; I denotes the infected individuals who are contagious; and R denote the recovered individuals who are not infectious any more and have acquired immunity againt further infection. More precisely $\int_m^{m+\Delta m} S(m',t)dm' \approx S(m,t)\Delta m$, represents the susceptible individuals with size in $[m, m+\Delta m]$ at time t. It is assumed that there is no vertical transmission so that all births will enter the susceptible class. It is also assumed that all transition rates can be size-dependent. Then, the initial-boundary-value problem for the simple size-structured SIR model with size-specific infection rate $\lambda(m)$, size-specific death rate $\theta(m)$ and size-specific recovery rate $\gamma(m)$ is given by the following nonlinear hyperbolic system of partial differential equa-

tions

$$\frac{\partial S}{\partial t} + g(m)\frac{\partial S}{\partial m} = -\lambda(t)b(m)S - \theta(m)S \tag{3.1}$$

$$\lambda(t) = \beta \int_{m_0}^{\infty} b(m')\frac{I(t,m')}{\eta(t,m)}dm' \tag{3.2}$$

$$\frac{\partial I}{\partial t} + g(m)\frac{\partial I}{\partial m} = \lambda(t)b(m)S - \gamma(m)I - \theta(m)I \tag{3.3}$$

$$\frac{\partial R}{\partial t} + g(m)\frac{\partial R}{\partial m} = \gamma(m)I - \theta(m)R \tag{3.4}$$

$$S(0,m) = S_0(m),\ \ I(0,m) = I_0(m),\ \ R(0,m) = R_0(m) \tag{3.5}$$

$$S(t,m_0) = \rho,\ \ I(t,m_0) = 0,\ \ R(t,m_0) = 0 \tag{3.6}$$

where ρ represents the assumed constant birth rate. In this model new infections occur at a proportionately-mixed size-dependent bilinear incidence rate with $b(m)$ denoting the size-specific activity level. The population is asymptotically constant, in other words, it is assumed that the total population $\eta(t,m) \equiv M(m)$, the stable size distribution.

3.1. The threshold quantity R_0 and steady state size distributions

The basic reproduction number for the SIR model (3.1) is

$$R_0 = \beta \int_{m_0}^{\infty} b(m') \int_{m_0}^{m'} \frac{b(\alpha)}{g(\alpha)} \exp\left(-\int_{\alpha}^{m} \frac{\gamma(\omega)}{g(\omega)}d\omega\right) d\alpha dm'. \tag{3.7}$$

In the expression for (3.7), $b(m)$ is the size-specific activity level, $\frac{1}{g(m)}$ the size-specific average time spent in size m, and $\exp\left(-\int_{\alpha}^{m} \frac{\gamma(\omega)}{g(\omega)}d\omega\right)$ represents the

probability of survival of an individual in the infected stage from size group α to size m, with $m_0 \leq \alpha \leq m$. Therefore R_0 represents the effective contacts of individuals from size m_0 to the highest size (here taking as ∞ for mathematical convenience) with infective individuals of all sizes.

Following the procedure described in Castillo-Chavez et al. [9], we can show that System (3.1) supports a disease-free non-uniform steady state distribution and endemic distributions. The disease free non-uniform steady state distribution is

$$\begin{aligned} S^{\diamondsuit}(m) &= \rho \exp\left(-\int_{m_0}^{m} \frac{\theta(m')}{g(m')} dm'\right), \\ I^{\diamondsuit}(m) &= 0, \\ R^{\diamondsuit}(m) &= 0. \end{aligned} \tag{3.8}$$

If we denote an endemic non-uniform steady state distribution by $\tilde{S}(m), \tilde{I}(m)$ and $\tilde{R}(m)$ with $\tilde{I}(m) > 0$ then at this state

$$\tilde{\lambda} = \beta \int_{m_0}^{\infty} b(m') \frac{\tilde{I}(m')}{\tilde{\eta}(m)} dm'. \tag{3.9}$$

Further if there exists a $\tilde{\lambda} > 0$ satisfying (3.9) (see Appendix A) then

$$\tilde{S}(m) = \rho \exp\left(-\int_{m_0}^{m} \frac{\tilde{\lambda} b(m') + \theta(m')}{g(m')} dm'\right) \tag{3.10}$$

$$\begin{aligned}\tilde{I}(m) &= \tilde{\lambda}\rho \exp\left(-\int_{m_0}^{m} \frac{\theta(m')}{g(m')} dm'\right) \int_{m_0}^{m} \frac{b(m')}{g(m')} \\ &\quad \exp\left(-\int_{m_0}^{m'} \frac{\tilde{\lambda} b(\alpha)}{g(\alpha)} d\alpha\right) \exp\left(-\int_{m'}^{m} \frac{\gamma(\alpha)}{g(\alpha)} d\alpha\right) dm'\end{aligned} \tag{3.11}$$

$$\tilde{R}(m) = \tilde{\eta}(m) - \tilde{S}(m) - \tilde{I}(m). \tag{3.12}$$

where

$$\tilde{\eta}(m) = \rho \exp\left(-\int_{m_0}^{m} \frac{\theta(m')}{g(m')} dm'\right) \tag{3.13}$$

and $\tilde{\lambda}$ is given in (3.9). Substituting $\tilde{I}(m)$ into equation (3.9) we obtain

$$\begin{aligned}\tilde{\lambda} &= \tilde{\lambda}\beta \int_{m_0}^{\infty} b(m') \int_{m_0}^{m'} \frac{b(\alpha)}{g(\alpha)} \exp\left(-\tilde{\lambda} \int_{m_0}^{\alpha} \frac{b(\omega)}{g(\omega)} d\omega\right) \\ &\quad \exp\left(-\int_{\alpha}^{m} \frac{\gamma(\omega)}{g(\omega)} d\omega\right) d\alpha dm'.\end{aligned} \tag{3.14}$$

Under the assumption $\tilde{\lambda} \neq 0$, from (3.14) we obtain the characteristic equation:

$$\begin{aligned}1 &= \beta \int_{m_0}^{\infty} b(m') \int_{m_0}^{m'} \frac{b(\alpha)}{g(\alpha)} \exp\left(-\tilde{\lambda} \int_{m_0}^{\alpha} \frac{b(\omega)}{g(\omega)} d\omega\right) \\ &\quad \exp\left(-\int_{\alpha}^{m} \frac{\gamma(\omega)}{g(\omega)} d\omega\right) d\alpha dm'.\end{aligned} \tag{3.15}$$

Let $H(\tilde{\lambda})$ denote the function on the RHS of equation (3.15). Then $H'(\tilde{\lambda}) = \left(-\int_{m_0}^{\alpha} \frac{b(\omega)}{g(\omega)} d\omega\right) H(\tilde{\lambda}) < 0$ for $\tilde{\lambda} \in (-\infty, \infty)$ and $\lim_{\tilde{\lambda} \to \infty} H(\tilde{\lambda}) = 0$ (if $b(\omega) \neq 0$). Thus, the equation $H(\tilde{\lambda}_c) = 1$ has a unique real solution $\tilde{\lambda}_c$. Note that $H(0) = R_0$.

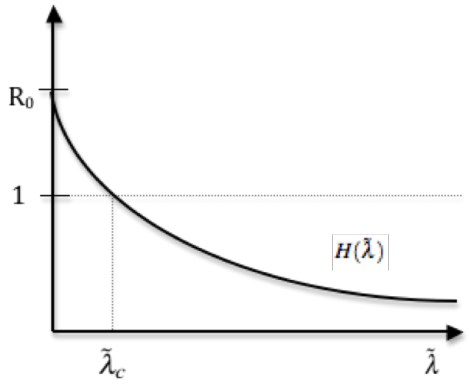

Figure 1: Solution of Characteristic Equation for $R_0 > 1$

Thus, $\tilde{\lambda} < 0$ (> 0) if $R_0 < 1$ (> 1) (see Figure 1). Therefore, an endemic steady state size distribution exists as long as $R_0 > 1$ and it is unique.

3.2. Stability of steady state size distributions

Let $E^* = (S^*, I^*, R^*)$ denote a steady state size distribution, and let

$$\lambda^* = \beta \int_{m_0}^{\infty} b(m') \frac{I^*(m')}{\eta^*(m)} dm'. \tag{3.16}$$

Now that we know that there exists a unique $\lambda^* > 0$, to determine the local stability of E^*, the following perturbations

$$\begin{aligned} S(t,m) &= S^*(m) + \zeta(t,m) && (3.17)\\ I(t,m) &= I^*(m) + \xi(t,m) && (3.18)\\ R(t,m) &= R^*(m) + \psi(t,m) && (3.19)\\ \lambda(t) &= \lambda^* + \delta(t) && (3.20) \end{aligned}$$

of the steady state are considered. Linearization leads (small perturbations) to the following first order approximate model for ζ, ξ, ψ and δ:

$$\begin{aligned} \frac{d\zeta}{dt} + g(m)\frac{d\zeta}{dm} &= -\lambda^* b(m)\zeta - \theta(m)\zeta - \delta(t)b(m)S^* && (3.21)\\ \frac{d\xi}{dt} + g(m)\frac{d\xi}{dm} &= \lambda^* b(m)\zeta - (\gamma(m) + \theta(m))\xi + \delta(t)b(m)S^* && (3.22)\\ \frac{d\psi}{dt} + g(m)\frac{d\psi}{dm} &= \gamma(m)\xi - \theta(m)\psi && (3.23)\\ \delta(t) &= \beta \int_{m_0}^{\infty} b(m')\frac{\xi(t,m')}{\eta^*(m')}dm' && (3.24)\\ \zeta(t,m_0) &= \xi(t,m_0) = \psi(t,m_0) = 0, && (3.25)\\ \zeta(0,m) &= S(0,m) - S^*(m), \xi(0,m) = I(0,m) - I^*(m),\\ \psi(0,m) &= R(0,m) - R^*(m). \end{aligned}$$

See Appendix B for details on how this approximation was obtained.

We study System (3.21)-(3.25), under separable perturbations, that is,

solutions of the form:

$$\begin{aligned}
\zeta(t,m) &= \hat{\zeta}(m)e^{pt} \\
\xi(t,m) &= \hat{\xi}(m)e^{pt} \\
\psi(t,m) &= \hat{\psi}(m)e^{pt} \\
\delta(t) &= \hat{\delta}e^{pt}
\end{aligned} \tag{3.26}$$

where $\hat{\delta}$ and p are constants. These solutions lead to the formal expressions

$$\begin{aligned}
\hat{\zeta}(m) &= -\hat{\delta}\rho \exp\left(-\int_{m_0}^{m} \frac{\theta(m')}{g(m')}dm'\right) \exp\left(-\int_{m_0}^{m} \frac{\lambda^* b(m')}{g(m')}dm'\right) \\
&\quad \int_{m_0}^{m} \frac{b(m')}{g(m')} \exp\left(-\int_{m'}^{m} \frac{p}{g(\alpha)}d\alpha\right)dm', \qquad (3.27) \\
\hat{\xi}(m) &= \hat{\delta}\rho \exp\left(-\int_{m_0}^{m} \frac{\theta(m')}{g(m')}dm'\right) \left\{\int_{m_0}^{m} \frac{b(m')}{g(m')} \exp\left(-\int_{m_0}^{m'} \frac{\lambda^* b(\alpha)}{g(\alpha)}d\alpha\right)\right. \\
&\quad \exp\left(-\int_{m'}^{m} \frac{\gamma(\alpha)}{g(\alpha)}d\alpha\right) \exp\left(-\int_{m'}^{m} \frac{p}{g(\alpha)}d\alpha\right) \\
&\quad \left.\left[1-\lambda^* \int_{m_0}^{m'} \frac{b(\alpha)}{g(\alpha)} \exp\left(-\int_{\alpha}^{m'} \frac{p}{g(\omega)}d\omega\right)d\alpha\right]dm'\right\}, \qquad (3.28)
\end{aligned}$$

$$\begin{aligned}
\hat{\psi}(m) &= \hat{\delta}\rho \exp\left(-\int_{m_0}^{m} \frac{p+\theta(m')}{g(m')}dm'\right) \int_{m_0}^{m} \frac{\gamma(m')}{g(m')} \left\{\int_{m_0}^{m'} \frac{b(\alpha)}{g(\alpha)}\right. \\
&\quad \exp\left(\int_{m_0}^{\alpha} \frac{p}{g(\omega)}d\omega\right) \exp\left(-\int_{m_0}^{\alpha} \frac{\lambda^* b(\omega)}{g(\omega)}d\omega\right) \exp\left(-\int_{\alpha}^{m'} \frac{\gamma(\omega)}{g(\omega)}d\omega\right) \\
&\quad \left.\left[1-\lambda^* \int_{m_0}^{\alpha} \frac{b(\omega)}{g(\omega)} \exp\left(-\int_{\omega}^{\alpha} \frac{p}{g(\varepsilon)}d\varepsilon\right)d\omega\right]d\alpha\right\}dm', \qquad (3.29) \\
\hat{\delta} &= \beta \int_{m_0}^{\infty} b(m) \frac{\hat{\xi}(m)}{\eta^*(m)}dm. \qquad (3.30)
\end{aligned}$$

From (3.28) and (3.30), assuming that $\hat{\delta}$ is not zero, we obtain the characteristic

equation:

$$
\begin{aligned}
1 \;=\; & \beta \int_{m_0}^{\infty} b(m) \left\{ \int_{m_0}^{m} \frac{b(m')}{g(m')} \exp\left(- \int_{m_0}^{m'} \frac{\lambda^* b(\alpha)}{g(\alpha)} d\alpha \right) \right. \\
& \exp\left(- \int_{m'}^{m} \frac{\gamma(\alpha)}{g(\alpha)} d\alpha \right) \exp\left(- \int_{m'}^{m} \frac{p}{g(\alpha)} d\alpha \right) \\
& \left. \left[1 - \lambda^* \int_{m_0}^{m'} \frac{b(\alpha)}{g(\alpha)} \exp\left(- \int_{\alpha}^{m'} \frac{p}{g(\omega)} d\omega \right) d\alpha \right] dm' \right\} dm, \quad (3.31)
\end{aligned}
$$

a transcendental equation for p.

If all solutions p Equation (3.31) have negative real parts, then all solutions of the form (3.26) will tend to zero as t goes to infinity, and the non-uniform steady state size distribution E^* will be stable.

To show the stability of the endemic equilibrium $\tilde{E}$, it requires to show that for $\lambda^* > 0$ the roots of Equation (3.31) have negative real parts. It turns out that this is very difficult to show. Numerical simulations suggest (ODE parallel system in Chapter 4) that this may be the case. The research in [9] includes the numerical analysis of the above characteristic equation in the presence of two activity levels and constant $\theta(m)$, seems to support our hypothesis.

For the disease-free equilibrium we have $\lambda^* = 0$, in which case (3.31) becomes:

$$
\begin{aligned}
1 \;=\; & \beta \int_{m_0}^{\infty} b(m) \left\{ \int_{m_0}^{m} \frac{b(m')}{g(m')} \exp\left(- \int_{m'}^{m} \frac{\gamma(\alpha)}{g(\alpha)} d\alpha \right) \right. \\
& \left. \exp\left(- \int_{m'}^{m} \frac{p}{g(\alpha)} d\alpha \right) dm' \right\} dm. \quad (3.32)
\end{aligned}
$$

Let $F(p)$ denote the function on the RHS of (3.32). It is easy to show that F is a decreasing function of p as $F'(p) < 0$. Note that $F(p) \to \infty$ as $p \to -\infty$ and $F(p) \to 0$ as $p \to \infty$. Thus, as before, Equation (3.32) has a unique real solution, which we denote by p^*. Note also that $F(0) = R_0$. Thus, $p^* < 0$ (> 0) if and only if $R_0 < 1$ (> 1).

Let $p = r \pm is$ be a complex solution of (3.32). Note that

$$\begin{aligned}
1 &= F(p) = |F(r+is)| \\
&= |\beta \int_{m_0}^{\infty} b(m) \int_{m_0}^{m} \frac{b(m')}{g(m')} \exp\left(-\int_{m'}^{m} \frac{\gamma(\alpha)}{g(\alpha)} d\alpha\right) \exp\left(-\int_{m'}^{m} \frac{r}{g(\alpha)} d\alpha\right) \\
&\quad (\cos\left(\int_{m'}^{m} \frac{s}{g(\alpha)} d\alpha\right) - i \sin\left(\int_{m'}^{m} \frac{s}{g(\alpha)} d\alpha\right)) dm' dm| \\
&\leq \beta \int_{m_0}^{\infty} b(m) \int_{m_0}^{m} \frac{b(m')}{g(m')} \exp\left(-\int_{m'}^{m} \frac{\gamma(\alpha)}{g(\alpha)} d\alpha\right) \exp\left(-\int_{m'}^{m} \frac{r}{g(\alpha)} d\alpha\right) \\
&\quad |\cos\left(\int_{m'}^{m} \frac{s}{g(\alpha)} d\alpha\right) - i \sin\left(\int_{m'}^{m} \frac{s}{g(\alpha)} d\alpha\right)| dm' dm \\
&= F(r)
\end{aligned}$$

Thus, $F(r) \leq F(p)$. Therefore, if $R_0 < 1$ then $r < p^* \leq 0$. It follows that the trivial steady-state is locally asymptotically stable if $R_0 < 1$, and it is unstable if $R_0 > 1$. Then the summary of our results is the following:

Theorem 3.1

- *If $R_0 < 1$ then the disease-free steady state is locally asymptotically stable.*

- *If $R_0 > 1$ then the disease free steady state is unstable and an unique endemic seady state exists.*

3.3. Conclusions

Chapter 3 builds a SIR epidemiological model under an explicit size-structure framework. We prove the existence (under some conditions) of an endemic state and establish the stability of the non-uniform infection-free size distribution when $R_0 < 1$, while showing that it becomes unstable when $R_0 > 1$.

CHAPTER 4

SYSTEM OF N ORDINARY DIFFERENTIAL EQUATIONS

The data available for the vital rates (fertility, growth and mortality) is usually given for size ranges. Therefore, it makes sense to find a framework that makes use of a finite number of size classes. A nonlinear system of ordinary differential equations is derived from first principles that allows for the study of the dynamics of size-structured populations that are growing or decaying exponentially. The epidemiologic structure for each class consists of individuals that are in the states of susceptible, infectious and recovered.

The approach divides the population density in n size groups defined by the size intervals $[m_{i-1}, m_i]$ where $0 = m_0 < m_1 < m_2 < ... < m_{n-1} < m_n = \infty$. It is convenient to let $[0, m_1]$ include all individuals with size smaller than m_1 and $[m_{n-1}, \infty)$ all individuals over size m_{n-1}.

We assume that the population has reached the stable non-uniform size distribution with growth $g(= 0, > 0, < 0)$, $\eta(t,m) = e^{qt}M(m)$. We further assume that death, growth and fertility rates are constant for m in $[m_{i-1}, m_i]$ with $\theta(m) = \theta_i, g(m) = g_i, f(t,m') = f_i$.

The number of individuals in the size group $[m_{i-1}, m_i]$ is given by

$$N_i(t) = \int_{m_{i-1}}^{m_i} \eta(t,m)dm = e^{qt} \int_{m_{i-1}}^{m_i} M(m)dm = e^{qt}N_i \tag{4.1}$$

where N_i is the size of the $i-$th size group at time 0.

Then, from

$$\eta(t,m_0) = e^{qt}M_0 = \int_{m_0}^{\infty} f(m')\eta(t,m')dm' = \sum_{i=1}^{n} f_i e^{qt} \int_{m_{i-1}}^{m_i} M(m)dm = \sum_{i=1}^{n} f_i e^{qt} N_i$$

we have $e^{qt}M_0 = \sum_{i=1}^{n} f_i e^{qt} N_i$ and thus

$$M_0 = \sum_{i=1}^{\infty} f_i N_i.$$

From (2.2), integrating for $m \in [m_{i-1}, m_i]$ yields

$$\int_{m_{i-1}}^{m} \frac{dM}{M} = \int_{m_{i-1}}^{m} \frac{-(q+\theta_i)}{g_i} dm$$

or

$$M(m) = M(m_{i-1}) \exp\left(\frac{-(q+\theta_i)}{g_i}(m - m_{i-1}) \right). \tag{4.2}$$

Now, since $N_i = \int_{m_{i-1}}^{m_i} M(m)dm$, using (4.2) we have

$$\begin{aligned} N_i &= \int_{m_{i-1}}^{m_i} M(m_{i-1}) \exp\left(\frac{-(q+\theta_i)}{g_i}(m - m_{i-1}) \right) \\ &= M(m_{i-1}) g_i \left[\frac{1 - \exp\left(\frac{-(q+\theta_i)}{g_i}(m_i - m_{i-1}) \right)}{q+\theta_i} \right] \end{aligned} \tag{4.3}$$

For $i = 1,2,3,...,n-1$ it is convenient to define the constants c_i by $M(m_i) = c_i N_i$

$$\begin{aligned} c_i &= \frac{M(m_i)}{N_i} \qquad (4.4) \\ &= \frac{M(m_{i-1})\exp\left(\frac{-(q+\theta_i)}{g_i}(m_i - m_{i-1})\right)}{M(m_{i-1})g_i\left[\frac{1-\exp\left(\frac{-(q+\theta_i)}{g_i}(m_i-m_{i-1})\right)}{q+\theta_i}\right]} \\ c_i &= \frac{q+\theta_i}{g_i\exp\left(\frac{q+\theta_i}{g_i}(m_i - m_{i-1})\right) - 1}. \qquad (4.5) \end{aligned}$$

Integration of (2.1) in the interval $[m_{i-1}, m_i]$ and equation (4.1) gives

$$\begin{aligned} \frac{\partial \eta}{\partial t} + g(m)\frac{\partial \eta}{\partial m} &= -\theta(m)\eta \\ \int_{m_{i-1}}^{m_i} \frac{\partial \eta}{\partial t} dm + \int_{m_{i-1}}^{m_i} g(m)\frac{\partial \eta}{\partial m} dm &= -\theta_i \int_{m_{i-1}}^{m_i} \eta dm \\ \frac{\partial \int_{m_{i-1}}^{m_i} \eta dm}{\partial t} + (g_i\eta(t,m_i) - g_{i-1}\eta(t,m_{i-1})) &= -\theta_i \int_{m_{i-1}}^{m_i} \eta dm \\ \frac{dN_i}{dt} + (g_i\eta(t,m_i) - g_{i-1}\eta(t,m_{i-1})) &= -\theta_i N_i \\ \frac{dN_i}{dt} + (e^{qt}g_i M(m_i) - e^{qt}g_{i-1}M(m_{i-1})) &= -\theta_i N_i \\ \frac{dN_i}{dt} + (g_i c_i e^{qt} N_i - g_{i-1}c_{i-1}e^{qt}N_{i-1}) &= -\theta_i N_i \\ \frac{dN_i}{dt} + (g_i c_i N_i - g_{i-1}c_{i-1}N_{i-1}) &= -\theta_i N_i \end{aligned}$$

Thus,

$$\frac{dN_i}{dt} = -(\theta_i + g_i c_i)N_i + g_{i-1}c_{i-1}N_{i-1}, \quad \texttt{for} \quad i = 1,2,...,n-1 \qquad (4.6)$$

More specifically, the N_1 equation is

$$\begin{aligned}
\frac{dN_1}{dt} &= -(\theta_1 + g_1 c_1)N_1 + c_0 N_0 \\
&= -(\theta_1 + g_1 c_1)N_1 + e^{qt} M(m_0) \\
&= -(\theta_1 + g_1 c_1)N_1 + \sum_{i=1}^{n} f_i N_i e^{qt} \\
&= -(\theta_1 + g_1 c_1)N_1 + \sum_{i=1}^{n} f_i N_i \\
\frac{dN_1}{dt} &= \sum_{i=1}^{n} f_i N_i - (\theta_1 + g_1 c_1)N_1. \qquad (4.7)
\end{aligned}$$

Because c_i represents the transfer rate constants between successive size groups and we are assuming n is the last age group or the "biggest" possible size, we have $c_n \approx 0$. Therefore the set of n-ODE's that represents the sized structure population in n subgroups become:

$$\begin{aligned}
\frac{dN_1}{dt} &= \sum_{i=1}^{n} f_i N_i - (\theta_1 + g_1 c_1)N_1 \\
\frac{dN_i}{dt} &= -(\theta_i + g_i c_i)N_i + g_{i-1} c_{i-1} N_{i-1}, \quad \texttt{for} \quad i = 2, ..., n-1 \qquad (4.8) \\
\frac{dN_n}{dt} &= -\theta_n N_n + g_{i-1} c_{n-1} N_{n-1}.
\end{aligned}$$

For the case of constant population the term $g_0 \sum_{i=1}^{n} f_i N_i$ is just a constant that will be called ρ from now on. It is within the above framework that we will proceed to study disease dynamics numerically using *SIR* frameworks in the next section.

4.1. SIR: Derivation of a System of $3n$ Ordinary Differential Equations

Using the model described by (3.1)-(3.4), the derivation of a system of a $3n$ ordinary differential equations follows the framework in Hethcote [13]. It is assume that the $i-$th subscript denote the S,I,R classes in the $i-$th size interval $[m_{i-1},m_i]$. The transmission rate is assumed to be constant in eanch internal, i.e., $b(m)=b_i$ for $m\in[m_{i-1},m_i]$. Then, using $S(m_i)=c_iS_i, I(m_i)=c_iI_i$, $R(m_i)=c_iR_i$ and boundary condition in (2.1), we can integrate (3.1)-(3.4) on the size intervals $[m_{i-1},m_i]$ to obtain the initial-value problem, describe below, for a set of $3n$ ordinary differential equations.

Specifically, if we let $N_i=S_i+I_i+R_i$. then the equations for $m\in[m_{i-1},m_i]$ are given by

$$\begin{aligned}
\frac{\partial S_i}{\partial t}+g(m)\frac{\partial S_i}{\partial m} &= -\lambda_i b_i S_i-\theta_i S_i, && (4.9)\\
\frac{\partial I_i}{\partial t}+g(m)\frac{\partial I_i}{\partial m} &= \lambda_i b_i S_i-(\gamma_i+\theta_i)I_i, && (4.10)\\
\frac{\partial R_i}{\partial t}+g(m)\frac{\partial R_i}{\partial m} &= \gamma_i I_i-\theta_i R_i. && (4.11)
\end{aligned}$$

Given that $S(m_i)=c_iS_i$, we have

$$\begin{aligned}
g(m)\frac{\partial S_i}{\partial m} &= g_iS(m_i)-g_{i-1}S(m_{i-1})\\
&= g_ic_iS_i-g_{i-1}c_{i-1}S_{i-1}. && (4.12)
\end{aligned}$$

Since for $m \in [m_{i-1}, m_i]$

$$\lambda_i(t) = \beta \sum_{j=1}^{n} b_j \frac{I_j}{N_j}. \tag{4.13}$$

we see that

$$\frac{dS_i}{dt} = g_{i-1}c_{i-1}S_{i-1} - (\lambda_i b_i + g_i c_i + \theta_i)S_i.$$

As in the demographic model, the birth equation (**??**) becomes

$$\begin{aligned} S(m_0) &= \frac{\int_{m_0}^{\infty} \eta(m)dm}{\int_{m_0}^{\infty} \exp\left(-\int_{m_0}^{m'} \frac{\theta(m)}{g(m)}dm\right)dm'}, \\ c_0 S_0 &= \frac{\sum_{i=1}^{n} N_i}{\sum_{i=1}^{n} \exp\left(-\sum_{j=1}^{i} \frac{\theta_j}{g_j}\right)} = \rho, \end{aligned} \tag{4.14}$$

which is the case of constant population. Then similarly as for the demographic model we can divide de S_i epidemic classes in S_1 and S_i for $i \geq 2$, since all births are assumed to get into this class.

$$\begin{aligned} \frac{dS_1}{dt} &= c_0 S_0 - (\lambda_1 b_1 + g_1 c_1 + \theta_1)S_1, \\ &= \rho - (\lambda_1 b_1 + g_1 c_1 + \theta_1)S_1. \end{aligned} \tag{4.15}$$

$$\begin{aligned} \frac{dS_i}{dt} &= g_{i-1}c_{i-1}S_{i-1} - (\lambda_i b_i + g_i c_i + \theta_i)S_i, \quad \texttt{for} \quad i \geq 2. \\ &\lambda_i(t) = \beta \sum_{j=1}^{n} b_j \frac{I_j}{N_j}. \end{aligned}$$

Similarly for the $I(t,m)$ class, given $I(m_i) = c_i I_i$,

$$\begin{aligned} g(m)\frac{\partial I_i}{\partial m} &= g_i I(m_i) - g_{i-1} I(m_{i-1}) \\ &= g_i c_i I_i - g_{i-1} c_{i-1} I_{i-1} \end{aligned} \tag{4.16}$$

Thus from (4.10) with (4.16),

$$\frac{dI_i}{dt} = g_{i-1}c_{i-1}I_{i-1} + \lambda_i b_i S_i - (\gamma_i + \theta_i + g_i c_i)I_i.$$

These also have to be divided into I_1 and I_i for $i \geq 2$.

For I_1, the term $c_0 I_0 = 0$ because $I_0 = 0$ given the assumption that all births get into the S_1 class. Therefore,

$$\begin{aligned} \frac{dI_1}{dt} &= \lambda_1 b_1 S_1 - (\gamma_1 + \theta_1 + g_1 c_1)I_1, \\ \frac{dI_i}{dt} &= g_{i-1}c_{i-1}I_{i-1} + \lambda_i b_i S_i - (\gamma_i + \theta_i + g_i c_i)I_i, \quad \texttt{for} \quad i \geq 2. \end{aligned} \tag{4.17}$$

Following the same logic, for $R(t,m)$,

$$\begin{aligned} g(m)\frac{\partial R_i}{\partial m} &= g_i R(m_i) - g_{i-1}R(m_{i-1}) \\ &= g_i c_i R_i - g_{i-1}c_{i-1}R_{i-1}. \end{aligned} \tag{4.18}$$

From (4.11) with (cRm),

$$\frac{dR_i}{dt} = g_{i-1}c_{i-1}R_{i-1} + \gamma_i I_i - (\theta_i + g_i c_i)R_i.$$

As for I_1, R_1 the term $g_1 c_0 R_0 = 0$ because $R_0 = 0$ given the assumption that all births get into the S_1 class. Therefore,

$$\begin{aligned} \frac{dR_1}{dt} &= = \gamma_1 I_1 - (\theta_1 + g_1 c_1)R_1, \\ \frac{dR_i}{dt} &= g_{i-1}c_{i-1}R_{i-1} + \gamma_i I_i - (\theta_i + g_i c_i)R_i, \quad \texttt{for} \quad i \geq 2. \end{aligned} \tag{4.19}$$

The system of $3n$ ordinary differential equations is then $(4.15), (4.17)$, and (4.19). All this done with $q = 0$.

$$
\begin{aligned}
\frac{dS_1}{dt} &= \rho - (\lambda_1 b_1 + g_1 c_1 + \theta_1) S_1, \\
\frac{dS_i}{dt} &= g_{i-1} c_{i-1} S_{i-1} - (\lambda_i b_i + g_i c_i + \theta_i) S_i, \quad \texttt{for} \quad i \geq 2, \\
\frac{dS_n}{dt} &= g_{n-1} c_{n-1} S_{n-1} - (\lambda_n b_n + \theta_n) S_n, \\
& \lambda_i(t) = \beta \sum_{j=1}^{n} b_j \frac{I_j}{N_j}, \\
\frac{dI_1}{dt} &= \lambda_1 b_1 S_1 - (\gamma_1 + \theta_1 + g_1 c_1) I_1, \\
\frac{dI_i}{dt} &= g_{i-1} c_{i-1} I_{i-1} + \lambda_i b_i S_i - (\gamma_i + \theta_i + g_i c_i) I_i, \quad \texttt{for} \quad i \geq 2, \\
\frac{dI_n}{dt} &= g_{n-1} c_{n-1} I_{n-1} + \lambda_n b_n S_n - (\gamma_n + \theta_n) I_n, \\
\frac{dR_1}{dt} &= = \gamma_1 I_1 - (\theta_1 + g_1 c_1) R_1, \\
\frac{dR_i}{dt} &= g_{i-1} c_{i-1} R_{i-1} + \gamma_i I_i - (\theta_i + g_i c_i) R_i, \quad \texttt{for} \quad i \geq 2. \\
\frac{dR_n}{dt} &= g_{n-1} c_{n-1} R_{n-1} + \gamma_n I_n - \theta_n R_n.
\end{aligned}
\tag{4.20}
$$

This equivalent model, (4.20), assumes proportional mixing where b_i represents the size i activity level, β the probability of becoming infected per contact, g_i are the transfer rate between successive size groups or rate of leaving size i, c_i is a transfer scaling factor, θ_i is the mortality rate for size i group and γ_i is the size i recovery rate. All these rates are constants, which simplifies the analysis of the system. The function λ_i represents the effective contacts with

infected organisms of size group i. Once organisms reach maximal size n, they stay there until they die. This implies that transition rate for size n is zero. This model groups organisms in different size groups and facilitates the process of simulating.

4.2. SIR: Case $n = 2$

Given the complexity of the $3n$ ODE system we need to study the simplest version of it first to observe the dynamics. For the specific case of $n = 2$, where only two size classes are considered the model becomes

$$\begin{aligned}
\frac{dS_1}{dt} &= \rho - \left(\frac{\beta b_1^2}{N_1} I_1 + \frac{\beta b_1 b_2}{N_2} I_2 + g_1 c_1 + \theta_1\right) S_1, \\
\frac{dS_2}{dt} &= g_1 c_1 S_1 - \left(\frac{\beta b_2 b_1}{N_1} I_1 + \frac{\beta b_2^2}{N_2} I_2 + \theta_2\right) S_2, \\
\frac{dI_1}{dt} &= \frac{\beta b_1^2}{N_1} I_1 S_1 + \frac{\beta b_1 b_2}{N_2} I_2 S_1 - (\gamma_1 + \theta_1 + g_1 c_1) I_1, \\
\frac{dI_2}{dt} &= g_1 c_1 I_1 + \frac{\beta b_2 b_1}{N_1} I_1 S_2 + \frac{\beta b_2^2}{N_2} I_2 S_2 - (\gamma_2 + \theta_2) I_2, \\
\frac{dR_1}{dt} &= \gamma_1 I_1 - (\theta_1 + g_1 c_1) R_1, \\
\frac{dR_2}{dt} &= g_1 c_1 R_1 + \gamma_2 I_2 - \theta_2 R_2.
\end{aligned} \tag{4.21}$$

4.2.1. Threshold condition, R_0, for the ODE SIR model: Case $n = 2$

The disease free equilibrium (DFE) is $(S_1^*, S_2^*, I_1^*, I_2^*, R_1^*, R_2^*) = \left(\frac{\rho}{g_1c_1+\theta_1}, \frac{g_1c_1\rho}{\theta_2(g_1c_1+\theta_1)}, 0, 0, 0, 0\right)$. Then $N_1 = S_1 + I_1 + R_1 = \frac{\rho}{g_1c_1+\theta_1}$, $N_2 = S_2 + I_2 + R_2 = \frac{g_1c_1\rho}{\theta_2(g_1c_1+\theta_1)}$, and the total population is represented by $N = N_1 + N_2 = \frac{g_0\rho(g_1c_1+\theta_2)}{\theta_2(g_1c_1+\theta_1)}$.

Using the next generation matrix, the expression for the reproduction number, R_0, is

$$R_0 = \frac{1}{2}\left[\frac{\beta b_1^2}{\gamma_1 + g_1c_1 + \theta_1} + \frac{\beta b_2^2}{\gamma_2 + \theta_2} + \sqrt{\left(\frac{\beta b_1^2}{\gamma_1 + g_1c_1 + \theta_1} + \frac{\beta b_2^2}{\gamma_2 + \theta_2}\right)^2 + \frac{4\beta b_1 b_2 \theta_2}{(\gamma_2 + \theta_2)(\gamma_1 + g_1c_1 + \theta_1)}}\right] \quad (4.22)$$

The biological interpretation of R_0 is clear. The fraction $\frac{1}{\gamma_1+g_1c_1+\theta_1}$ represents the average amount of time that a member of group size 1 spends in the infected stage, and βb_1^2 is the effective contacts or infections of members of group size 1 with members of group size 1. Therefore, $\frac{\beta b_1^2}{\gamma_1+g_1c_1+\theta_1}$ are the new infections of members of group size 1 from infected organisms of that same size group. Similarly, $\frac{1}{\gamma_2+\theta_2}$ is the average time that a member of group size 2 spends in the infected stage and βb_2^2 is the infections of members of size group 2 with members of group size 2. Then, $\frac{\beta b_2^2}{\gamma_2+\theta_2}$ are the new infections of members of size group 2 from members of size group 2. The expression with the square root,

$\sqrt{\left(\frac{\beta b_1^2}{\gamma_1+g_1c_1+\theta_1}+\frac{\beta b_2^2}{\gamma_2+\theta_2}\right)^2+\frac{4\beta b_1 b_2\theta_2}{(\gamma_2+\theta_2)(\gamma_1+g_1c_1+\theta_1)}}$, represents the new infections of members of group size 1 with those in group size 2. Since all these interactions are counted twice the whole expression is multiplied by one half.

In order to determine the stability of the disease free equilibrium we computed the Jacobian and found the eigenvalues. The Jacobain matrix at the infection-free equlibrium has two negative eigenvalues, $-g_1c_1-\theta_1$ and $-\theta_2$, and two other eigenvalues given by the following quadratic equation

$$\lambda^2-(\beta b1^2-(\gamma_1+\theta_1+g_1c_1)+\beta b_2^2-(\theta_2+\gamma_2))\lambda+(\gamma_2+\theta_2)(\gamma_1+\theta_1+g_1c_1)$$
$$-\beta b_1^2(\gamma_2+\theta_2)-\beta b_2^2(\gamma_1+\theta_1+g_1c_1)-\beta b_1b_2\theta_2=0. \quad (4.23)$$

Thus, the disease free equilibrium is stable if the solutions of 4.23 have negative real parts. Using the Routh-Hurwitz criterion the conditions are:

$$\beta b1^2-(\gamma_1+\theta_1+g_1c_1)+\beta b_2^2-(\theta_2+\gamma_2) \;<\; 0, \quad (4.24)$$

$$(\gamma_2+\theta_2)(\gamma_1+\theta_1+g_1c_1)-\beta b_1^2(\gamma_2+\theta_2)$$
$$-\beta b_2^2(\gamma_1+\theta_1+g_1c_1)-\beta b_1b_2\theta_2 \;>\; 0. \quad (4.25)$$

These conditions hold if $R_0<1$. Thus, when $R_0<1$ the DFE is stable and there is no outbreak. But for $R_0>1$ the DFE is unstable and there will be an outbreak. We have been unable to establish existence of an endemic equilibrium when $R_0>1$. However, the numerical simulations in Chapter 4 suggest that this is the

case when $n = 2$ and $n = 2$.

4.2.2. Simulations of SIR with Two Size Classes

4.2.2.1. *Higher Harvesting of Larger Fish*

In oder to perform the simulations we looked into gathering data from some fish disease but we were impressed by the lack of data and interest in this field. It seems like fish diseases and their progression is not that important for many people because in many cases the fish diseases do not cause a major population bottleneck nor fish diseases affect humans. This lack of interest gave us the opportunity to reflect about it. Disease viruses are mutating constantly and we may get fish diseases that could affect humans. But also, it is important to understand the ecological processes of our populations and how human interventions like the harvesting affect the disease dynamics of these populations.

In the simulations performed in this study the parameters used were assumed from the different papers that talked about Renibacterium salmoninarum on chinook salmon. Renibacterium salmoninarum is the bacteria that cause bacterial kidney disease on this salmon population. It is well-established in the Great Lakes of the United States and it is one of the most important bacterial diseases

among salmonids.The following table presents the parameters used for the simulations.

Initial Conditions	Value	Initial Conditions	Value
$N_1(0)$	1800000	$N_2(0)$	3200000
$S_1(0)$	1799500	$S_2(0)$	3199500
$I_1(0)$	500	$I_2(0)$	500
$R_1(0)$	0	$R_2(0)$	0
Parameter		Parameter	
b_1	0.33	b_2	0.30
g_1	0.04	g_2	0.03
θ_1	0.0014	θ_2	0.0008
γ_1	1/6	γ_2	1/6
h_1	0.0001	h_2	0.005
f_1	0.05	f_2	0.3
c_1	0.05		

TABLE 2: Initial Conditions and Parameters Values for Two Size Classes

The first case considers that the population is fed with as many fish as harvested to maintain the population constant. The fish introduced to the population are in the smallest size group and it is assumed that they are all susceptible. Since it is assumed that the transmission rate is higher for smaller fish and harvesting introduces more individuals to the smallest size group, harvesting is increasing the number of infected individuals in the endemic steady state as observed in 2b and 2d. If we separate the infected population by size we observe that the endemic equilibrium for the second size class is a little smaller, but the endemic equilibrium for the first size group is substantially bigger as observed in 2a. The final size distribution 2c switches given that the feeding of the population has a higher effect in the dynamics than the growth. This change in behavior of the size populations is also observed in 2e. The main observation in this case is that harvesting increases the number of infectives due to the way the population is fed to keep it constant.

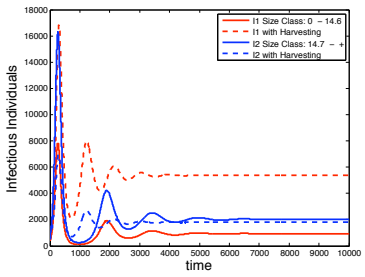

(a) Infectious individuals over time.

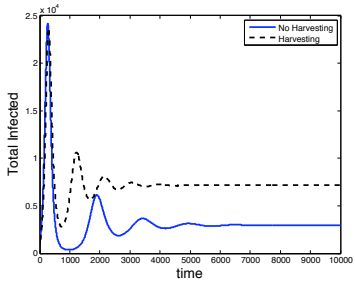

(b) Total infected over time.

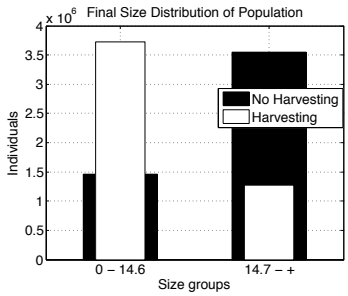

(c) Final distribution of population by size group.

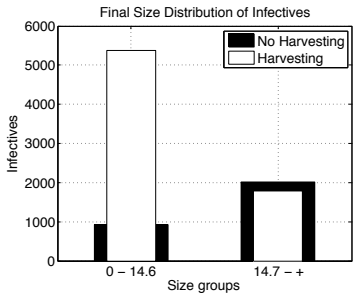

(d) Final distribution of infectives by size group.

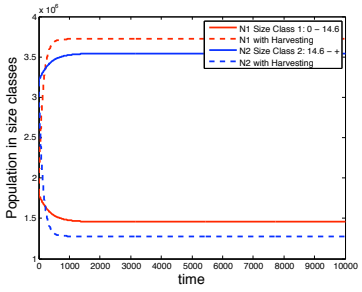

(e) Population dynamics for the two size groups. Population in this case is constant.

Figure 2: SIR Constant Population, 2 Size Classes

The second case considers a constant feeding of the population regardless of the number of individuals in the population and the number of individuals been harvested. New fish are introduced to the smallest class size and it is assumed that all of them are susceptible. Therefore, the term that expressed this process is $\sum f_n N_n(0) = f_1 N_1(0) + f_2 N_2(0)$. If the number of fish introduced is bigger than the number of fish that leave the population by death or harvesting, then the population grows, otherwise it decreases and goes to extinction. This is how the harvesting policies are established. It is obvious that without harvesting the population will stabilize in a higher number than with harvesting as observed in 3c, 3e and 3f, and as discussed in section 2.2. For the simulation in figures 3 it was considered a constant input that produced growth in the population and the harvesting just limited the growth. The total number of infected individuals was reduced as observed in 3b, but we can observe in 3d and 3a that this decrease was due to the reduction in the higher size class population given by the harvesting, while in the smallest size class the infection grew substantially. For this case, we can conclude that harvesting affected in a ”positive” way the infection by reducing the number of total infections in the population.

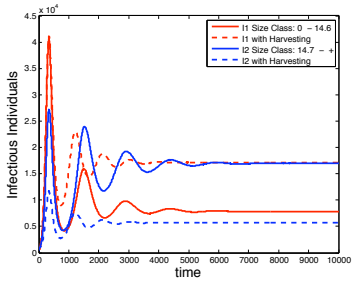

(a) Infectious individuals over time.

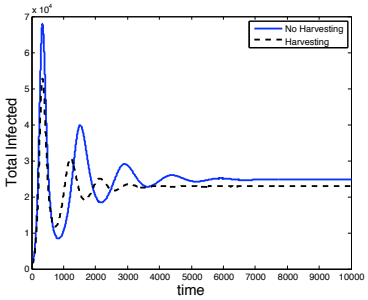

(b) Total infected over time.

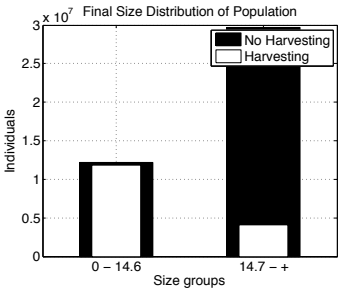

(c) Final distribution of population by size group.

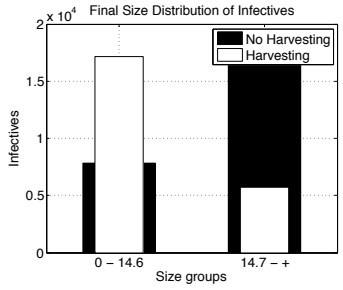

(d) Final distribution of infectives by size group.

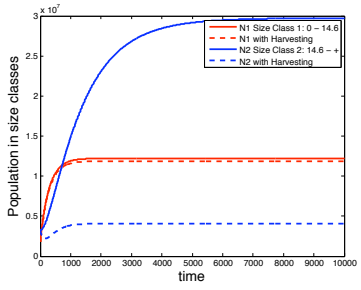

(e) Population dynamics for the two size groups.

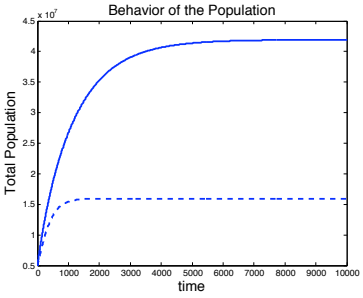

(f) Population dynamics.

Figure 3: SIR Constant Input, 2 Size Classes

The third case considers feeding proportional to the population, this is expressed as $f_1(S_1+I_1+R_1)+f_2(S_2+I_2+R_2)$ where S_1, S_2, I_1, I_2, R_1, and R_2 are not constant. The population will grow exponentially, but it will reach a stable size distribution in the proportion of the individuals in each size class. The effect of harvesting in this situation depends on the rates at which the population is been fed and the harvesting rates for the different classes. With harvesting, the population will grow exponentially but at a slower rate as observed in 4f. Harvesting is small in the smallest size class compared to the biggest size class, therefore the proportion of infectives at the end will be higher for size class one. For the second size class the final infectives proportion will be smaller given that many individuals are harvested 4a. Overall, although the number of infected individuals will be smaller with harvesting, the population will be smaller too and hence the proportion of infected individuals will be higher as shown in 4b.

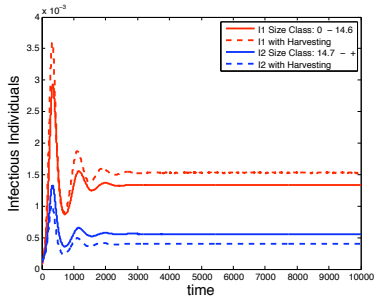

(a) Infectious individuals over time.

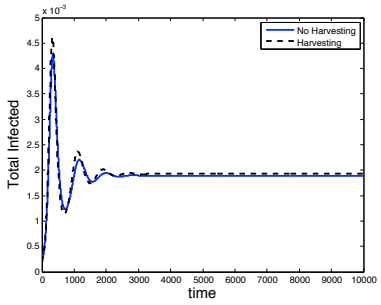

(b) Total infected over time.

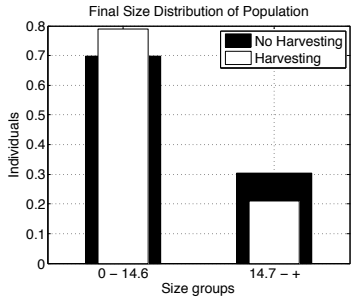

(c) Final distribution of population by size group.

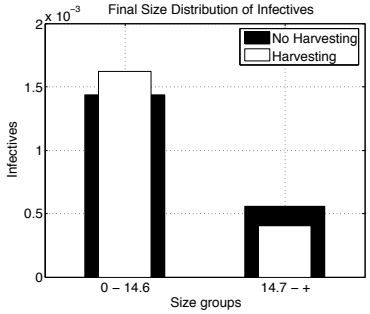

(d) Final distribution of infectives by size group.

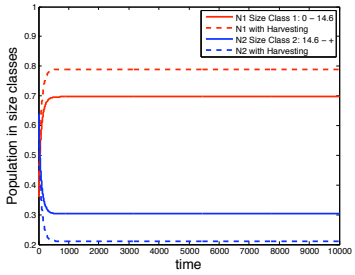

(e) Population dynamics for the two size groups.

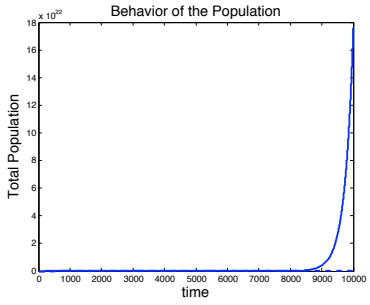

(f) Population dynamics.

Figure 4: SIR Unbounded Population, 2 Size Classes

4.2.2.2. *Higher Harvesting of Smaller Fish*

In this section an alternative way of harvesting is proposed with the purpose of examining how a change in harvesting policy during an outbreak affects the overall outcome of the disease. All conditions are the same as in the previous section 4.2.2.1 for the three cases, but instead of having a higher harvesting rate for bigger fish we are considering harvesting a bigger portion of the smaller fish. Since the transmission rate is higher for smaller fish, this may be a huge factor in the control of the disease.

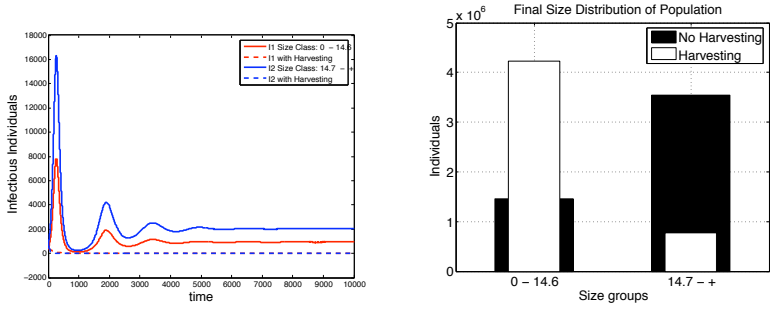

(a) Infectious individuals over time. (b) Final distribution of population by size group.

Figure 5: SIR Constant Population with Higher Size 1 Harvesting rate, 2 Size Classes

The graphs of the final distribution of the population by size group and the graph of the infectives dynamics for the two size groups are included

because they reflect the important effect of this new policy. It can be observed that the final population switches in numbers to more elements of the smaller size with harvesting. This change of harvesting policy shows that infected elements decrease fast and the system stabilizes in the disease free equilibrium. Therefore, it will be convenient to change harvesting policy as soon as an outbreak starts and therefore the disease it is controlled.

The second case considers when there is constant feeding of the population, but now with higher harvesting rate in the first class than in the second.

It can be observed that this harvesting strategy decreases considerably the population size. But it also controls the disease by reducing considerably the number of infections in the first size class. It may be a good strategy if it is implemented at the moment of the outbreak and for a short term since the decrease in the population is really big.

The third case considers when there is proportional feeding to the existing population, which produces population explosion, but with higher harvesting rate in the first class than in the second. The graph of the infected individuals over time 7a shows that with this strategy the infected individuals go to the zero steady state. Again as in the constant population case with this new

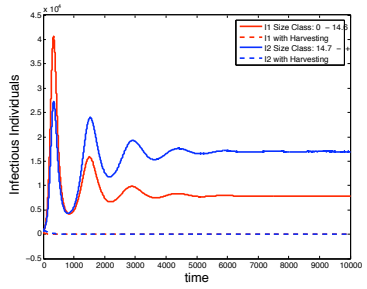

(a) Infectious individuals over time.

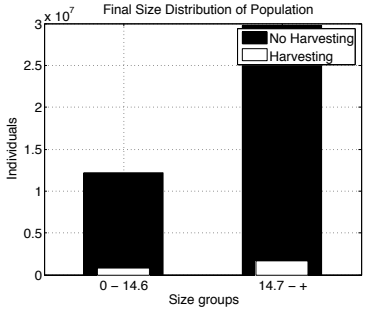

(b) Final distribution of population by size group.

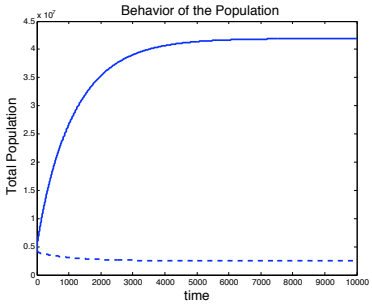

(c) Population dynamics.

Figure 6: SIR Constant Input with Higher Size 1 Harvesting rate, 2 Size Classes

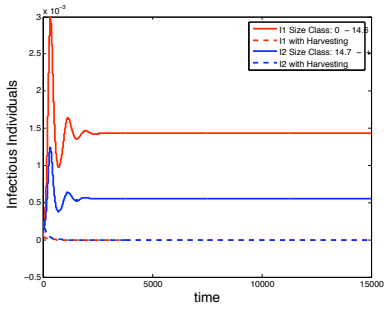

(a) Infectious individuals over time.

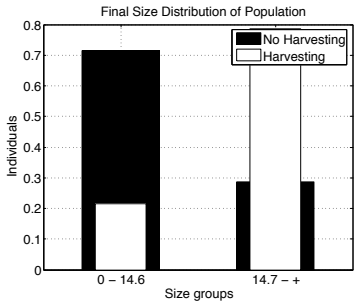

(b) Final distribution of population by size group.

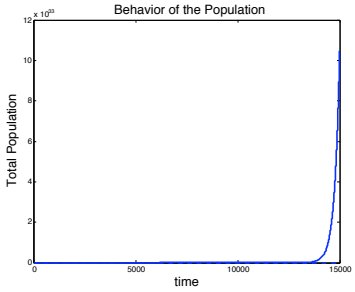

(c) Population dynamics.

Figure 7: SIR Unbounded Population with Higher Size 1 Harvesting Rate, 2 Size Classes

strategy, the population proportions of size switch but in this case there will be more elements in the second size group which makes sense since the population is growing exponentially and the harvesting is made mostly in the first class.

In all of the cases considered for the higher harvesting rate in the first size group presented control of the disease rapidly which means that in the case of an outbreak it is a good strategy to harvest massively the smaller fish. This policy can be implemented for a limited time until disease is controlled. In terms of numbers, with multiple simulations it was found that there is a threshold value for the harvesting rate of the first size group (h_1) between 0.03 and 0.04, for which the infectives go from endemic to extinct.

In the simulations with two size classes we observed that with the typical harvesting approach where larger fish are harvested in a higher rate the infections increased regardless of the way the population was fed. This phenomenon happens because the smaller fish population is increased since new fish come into the population in the smallest size group and smaller fish have higher susceptibility to disease as supported by research, [2], [23], [1], [3], [20]. The strategy of harvesting smaller fish in a higher rate and reducing considerably the harvesting of larger fish in all the cases produces extinction of the disease. This strategy is recommended for a small time period since the disease goes to

extinction fast and continuing with this strategy produces great reduction of the population in general. Therefore, simulations suggest that harvesting smaller fish during an outbreak is a good strategy to control de disease and once it is eradicated from the population usual harvesting policies can be resumed.

In this section, several harvesting strategies of a fish population are discussed and their influence in both the total population size and the disease control are presented. Two harvesting policies are considered, one with a higher harvesting rate of the smaller size and the other one with a higher harvesting rate of the larger size. Under each of the harvesting policies, three different scenarios in terms of the feeding rate of fish into the population are examined. The impact of harvesting is illustrated by comparing the population consequence with and without harvesting, which are shown in Figures 2-7. The following observations can be made. In the case of constant total population size, although a higher harvesting rate of smaller fish makes it more likely to control the disease (see Figures 2a and 5a) it also reduces the total population size of higher size (see Figures 2c and 5b). The impact on the total population size when harvesting smaller fish is much greater in the case of a constant feeding rate (see Figures 3c and 6b). Particularly, we observe that the total population is near extinction as

shown in Figure 6b, which suggests that this policy should be avoided. Finally, in the case of proportional feeding, more harvesting of smaller fish will help not only eliminate the disease (see Figures 4a and 7a) but also maintain the total population with a higher fraction of larger fish (see Figures 4b and 7b). Thus, the last scenario seems to be more beneficial.

4.3. Simulations of SIR with Three Size Classes

4.3.0.3. *Higher Harvesting of Larger Fish*

For the simulations with three class sizes or $n = 3$, we considered the same three cases as with two size classes. The parameters used for the simulations were again assumed from the different papers that we read through this study. The following table presents the parameters used for the simulations.
In the first case, the population is constant and the same number of harvested elements are introduced in the population into the first size class. Fish coming into the population do not have the disease and transmission rate for smaller fish is higher. Observations in this case are consistent with the simulations for two sizes. Since harvesting is increasing the smaller size class, because inflow into this compartment is equivalent to the total number of elements harvested in the population, and transmission rate is higher for this class, the number of

Initial Conditions	Value	Initial Conditions	Value
$N_1(0)$	1800000	$N_2(0)$	3200000
$S_1(0)$	1799500	$S_2(0)$	3199500
$I_1(0)$	500	$I_2(0)$	500
$R_1(0)$	0	$R_2(0)$	0
Parameter		Parameter	
b_1	0.33	b_2	0.30
g_1	0.04	g_2	0.03
θ_1	0.0014	θ_2	0.0008
γ_1	1/6	γ_2	1/6
c_1	0.05	c_2	0.04
h_1	0.0001	h_2	0.002
h_3	0.003	f_1	0
f_2	0.05	f_3	0.3

TABLE 3: Initial Conditions and Parameters Values for Three Size Classes

infected individuals in the endemic steady state is increasing as well 8b, 8d. As size increases the number of infected members in the endemic equilibrium, with harvesting, decreases 8a. Again, final size distribution demonstrates that the way the population is been fed has a bigger effect than the growth 8c, 8e. It can be concluded that in this case where the incoming flow is the same as the total of harvested elements the infection increases and the final distribution of infectives is decreasing by size.

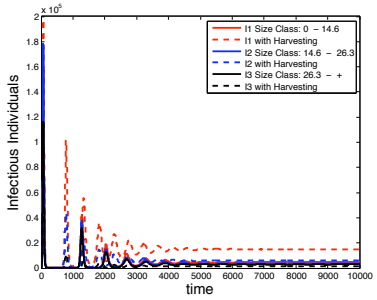

(a) Infectious individuals over time.

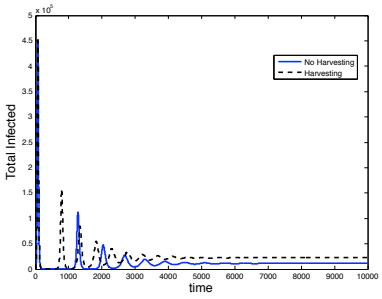

(b) Total infected over time.

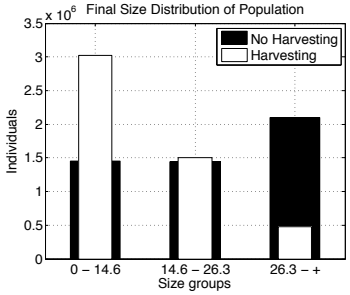

(c) Final distribution of population by size group.

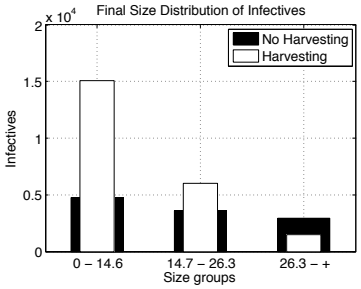

(d) Final distribution of infectives by size group.

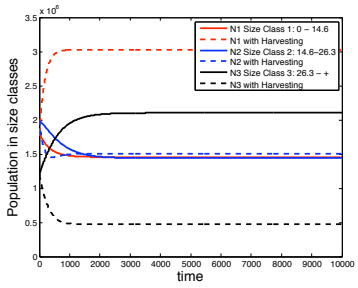

(e) Population dynamics for the three size groups. Population in this case is constant.

Figure 8: SIR Constant Population, 3 Size Classes

The second case, where there is a constant number of elements been introduced into the population, also assumes that new fish gets into the first size susceptible class. As in the two size simulations if the constant inflow is higher than the number of elements leaving the population the population grows, otherwise dies out. Population stabilizes at a higher number without harvesting than with harvesting as discussed before and observed in 9c, 9e, and 9f. In general, the number of infectives decreases 9b, but infection grows in the first size class and it is reduced in the other classes due to the harvesting 9a, 9d. Therefore we conclude that under the conditions of this case, the disease is reduced by the harvesting.

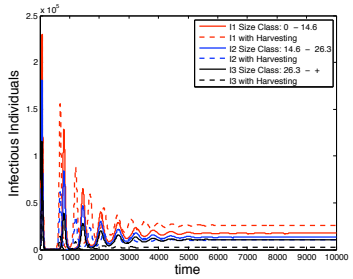

(a) Infectious individuals over time.

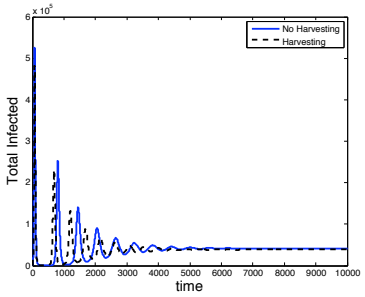

(b) Total infected over time.

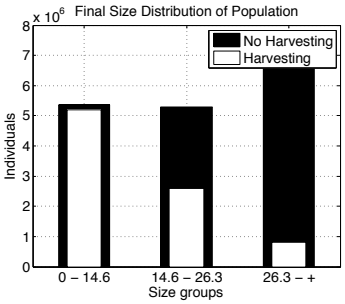

(c) Final distribution of population by size group.

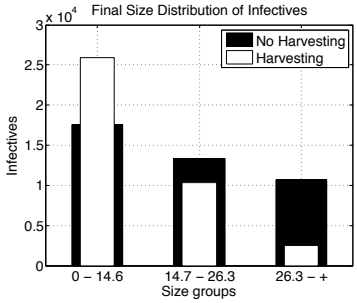

(d) Final distribution of infectives by size group.

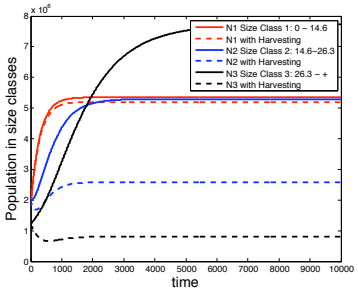

(e) Population dynamics for the three size groups.

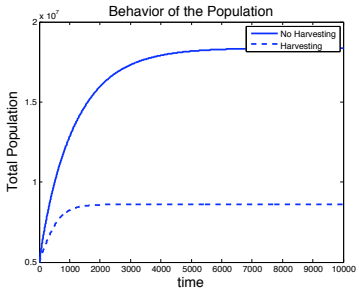

(f) Population dynamics.

Figure 9: SIR Constant Input, 3 Size Classes

Third case has inflow proportional to the existing population. This population grows exponentially and we can only analyze and observe what happens with the proportions of the individuals in each size class with respect to the total population at that moment, which stabilizes. With harvesting the population grows at a slower pace 10f. In contrast with the two size classes, the number of infected individuals in the final distribution is decreased 10b, 10d. This behavior is attributed to the different fertility rates for the different size classes.

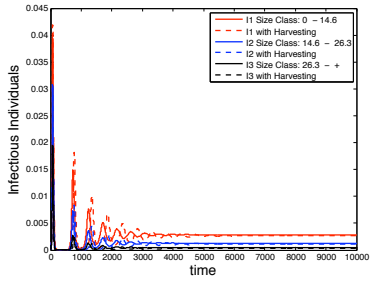

(a) Infectious individuals over time.

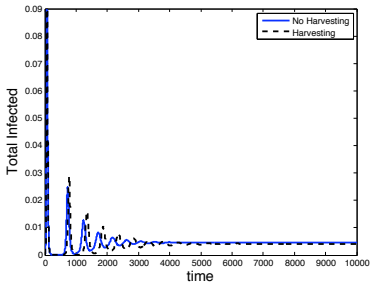

(b) Total infected over time.

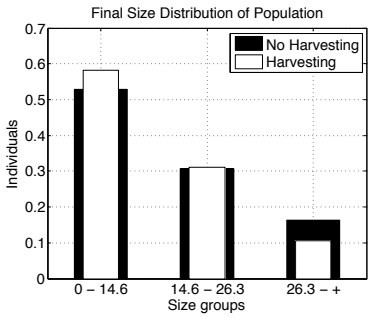

(c) Final distribution of population by size group.

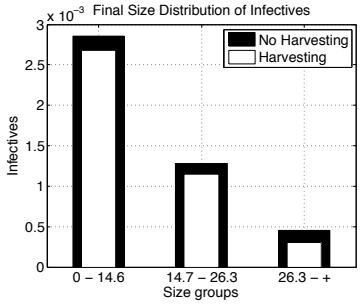

(d) Final distribution of infectives by size group.

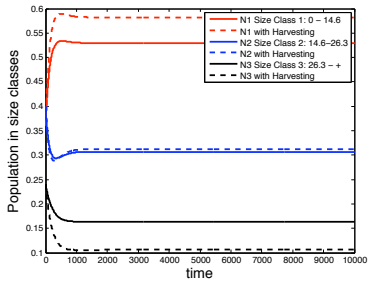

(e) Population dynamics for the three size groups.

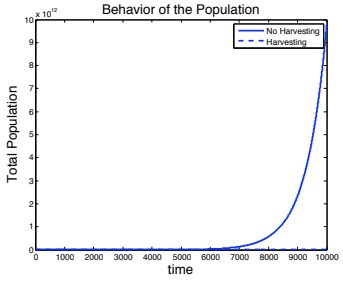

(f) Population dynamics.

Figure 10: SIR Unbounded Population, 3 Size Classes

4.3.0.4. *Higher Harvesting of Smaller Fish and Decreasing Rates with Size*

In order to understand better the effect of the harvesting policy in the outbreak of a disease and to propose different alternatives to control an outbreak two different harvesting approaches are presented. In this section the new harvesting rates propose a higher harvesting of smaller fish and decreasing rates as size increases. All conditions are the same as in the previous section 4.3.0.3 for the three cases.

In this first case, important changes happen on the dynamics of the population as observed in 11a and 11b. The infectives are reduced rapidly with the new harvesting strategy as observed in 11a. The population final distribution shows that after some time the population is mostly of the first size group, this is given by the way the population is fed. Therefore, as in the case of two size classes this new policy may be a good one to control the disease.

In the second case, the increment in harvesting of the smaller fish made a drastic effect on the population. Instead of the population growing as before we can observe that the population is greatly reduced 12c. If the harvesting rate for the first size group is increased more this will cause the extinction of the population and therefore the strategy is not viable.

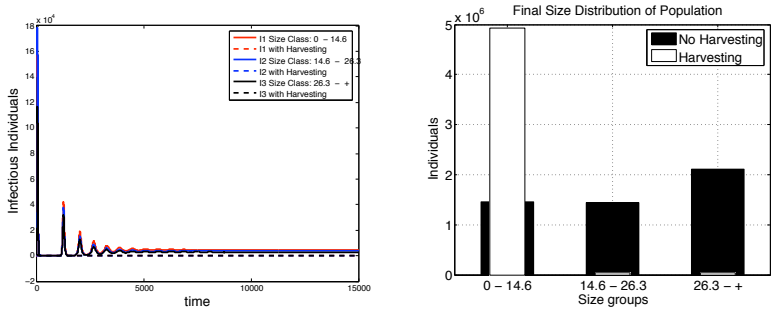

(a) Infectious individuals over time. (b) Final distribution of population by size group.

Figure 11: SIR Constant Population with Decreasing Harvesting Rate as Size Increases, 3 Size Classes

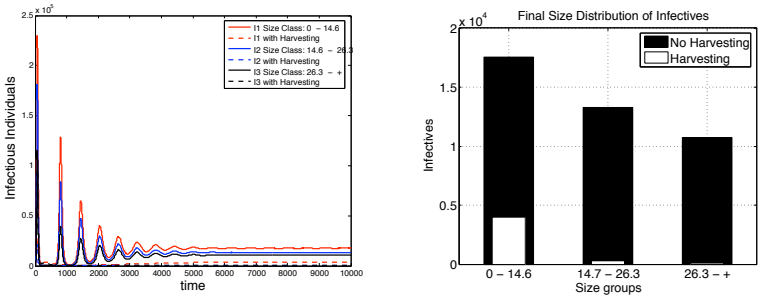

(a) Infectious individuals over time. (b) Final distribution of infectives by size group.

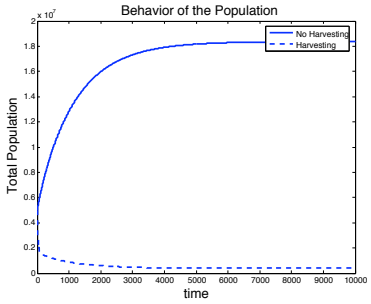

(c) Population dynamics.

Figure 12: SIR Constant Input, 3 Size Classes

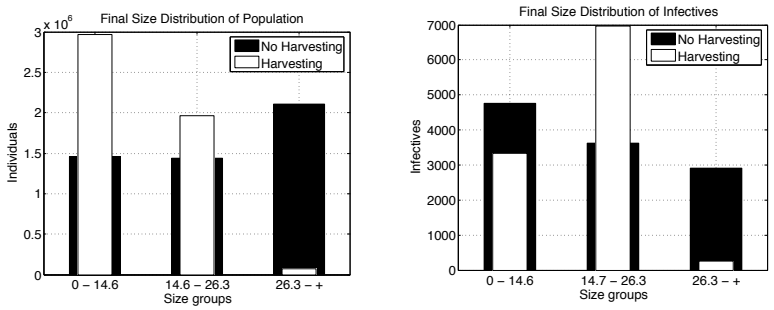

(a) Final distribution of population by size group.

(b) Final distribution of infectives by size group.

Figure 13: SIR Constant Population with Alternating Harvesting rates, 3 Size Classes

4.3.0.5. *Higher Harvesting of Smaller Fish in Alternating Pattern*

In this section the harvesting strategy proposed is an alternating rate policy, where the smaller class has a high harvesting rate, then second size class has a smaller harvesting rate and finally the third class has a high harvesting rate too. In this case we observe a bigger disease outbreak in the second size class 13b which is a consequence of the increment of the final population size on that size group. Overall, this strategy does not seems to help in controlling the disease outbreak.

In the second case the results were similar to the ones on 4.3.0.4 with the strategy of decreasing harvesting rates. The population is largely affected in a

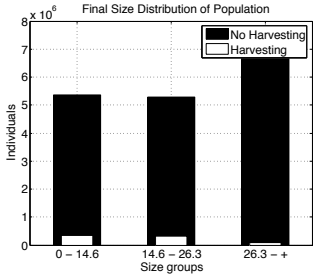

(a) Final distribution of population by size group.

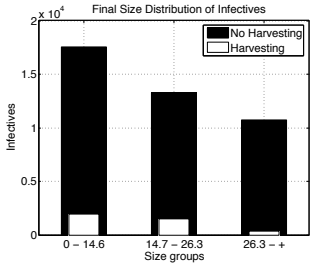

(b) Final distribution of infectives by size group.

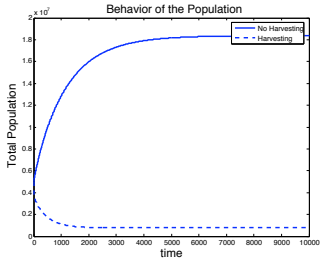

(c) Population dynamics.

Figure 14: SIR Constant Input with Alternating Harvesting Rates, 3 Size Classes

negative way and the disease is not eradicated for which we rule out this policy as a possibility to control the disease.

Similarly to the case with two size classes, when we consider three size classes we observe that harvesting increases the number of infections in the population regardless of the way it is fed. This is again attributed to the fact that smaller fish have higher susceptibility to diseases. It is also observed that implementing the strategy of harvesting more small fish and almost no large fish reduces completely the disease in a short period of time, for which it is a

good strategy to control the disease. But as in the previous case, this harvesting policy should not be held for a long time since it reduces the overall population considerably in the cases where population is not constant. These simulations suggest that modifying harvesting policies during an outbreak is a good way of controlling the disease.

In this section, several harvesting strategies of a fish population are discussed for a population stratified in three size classes. We observe their influence in both the total population size and the disease control. Three harvesting policies are considered, one with a higher harvesting rate of the smaller size, one with a higher harvesting rate of the larger size and one with higher harvesting or smaller and larger fish and low harvesting of middle size class fish. Under each of these harvesting policies, two different scenarios in terms of the feeding rate of fish into the population are examined. The impact of harvesting is illustrated by comparing the population consequence with and without harvesting, which are shown in Figures 8-14. The following observations can be made. In the case of constant total population size, although a higher harvesting rate of smaller fish makes it more likely to control the disease (see Figures 8a and 11a) it also reduces the population size of the bigger fish (see Figure 8c and 11b). The third

harvesting strategy with alternating harvesting rates just produces a reduction in the infections in the first and third size groups (see Figure 13b). The impact on the total population size when harvesting smaller fish is much greater in the case of a constant feeding rate (see Figures 9f and 12c). Particularly, we observe that the total population is extremely small as shown in Figure 12c, which suggests that this policy should be avoided. For the third harvesting strategy with alternating harvesting rates, with high harvesting rate of small and large fish, we observed similar results to the case of constant feeding where the population is near extinction (see Figures 14). Then, this last scenario seems to be more beneficial but for a limited time.

4.4. SI [Susceptible-Infective] ODE System

Since in many instances individuals of populations in the wild that become infected may actually not recover. We proceed to simulate, using the same ODE framework, disease dynamics on a S-I framework.

Similar to the SIR model, the $i-$th subscript denote the S,I classes in the ith size interval $[m_{i-1}, m_i]$ and transmission occurs by a proportionately-mixed size-dependent bilinear incidence rate $b(m) = b_i$ in that size range. The initial-value problem for a set of $2n$ ordinary differential equations, where n is the number of

size groups, is:

$$\begin{aligned}
\frac{dS_1}{dt} &= \rho - (\lambda_1 b_1 + g_1 c_1 + \theta_1) S_1 \\
\frac{dS_i}{dt} &= g_{i-1} c_{i-1} S_{i-1} - (\lambda_i b_i + g_i c_i + \theta_i) S_i \\
\lambda_i(t) &= \beta \sum_{j=1}^{n} b_j \frac{I_j}{N_j} \\
\frac{dI_1}{dt} &= \lambda_1 b_1 S_1 - (\theta_1 + g_1 c_1) I_1 \\
\frac{dI_i}{dt} &= g_{i-1} c_{i-1} I_{i-1} + \lambda_i b_i S_i - (\theta_1 + g_i c_i) I_i
\end{aligned} \tag{4.26}$$

Since this is a complex model, we tried to calculate the steady states of the case when only two size classes are considered. But we were only able to find an explicit solution for the disease free equilibrium (DFE) which is the same as in the SIR:

$$[S_1, S_2, I_1, I_2] = \left[\frac{\rho}{g_1 c_1 + \theta_1}, \frac{g_1 c_1 \rho}{\theta_2 (g_1 c_1 + \theta_1)}, 0, 0 \right]. \tag{4.27}$$

Then, we proceeded to perform some simulations with the same cases taken into consideration in 3.

4.4.1. SI Case $n = 2$: Simulations with Higher Harvesting of Larger Fish

In the simulations for SI we used the same parameters as in the SIR model 4.2.2.1 and 4.3.0.3. The first case considers that the population is fed with as

many fish as harvested to maintain the population constant. The fish introduced to the population are in the smallest size group and it is assumed that they are all susceptible. In this case, the harvesting reduces significantly the infections in the second size group and increase them in the first size group as observed in 15a and 15d. This is reasonable because many elements are harvested in the second size group and same number are introduced into the first size class as susceptible. This behavior of the infectious is driven by the behavior in the population as observed in 15c and 15e, but the number of infections is not significantly reduced as observed in 15b.

The second case considers a constant feeding of the population independent of the number of individuals in the population. New fish are introduced to the smallest susceptible class size with a term expressed by $\sum f_n N_n(0) = f_1 N_1(0) + f_2 N_2(0)$.

In this case, harvesting reduced greatly the population as presented in 16c, and 16e. The second size class is reduced more than the first class by the harvesting. This decrease in the population also determined the behavior in the infectious population 16a, 16b, and 16d.

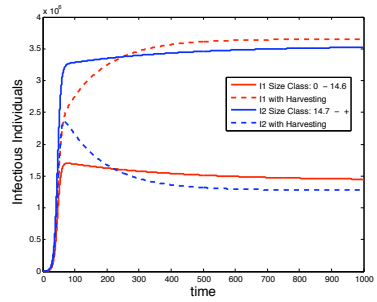

(a) Infectious individuals over time.

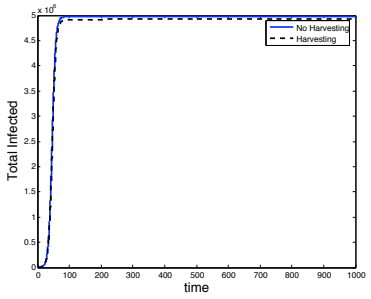

(b) Total infected over time.

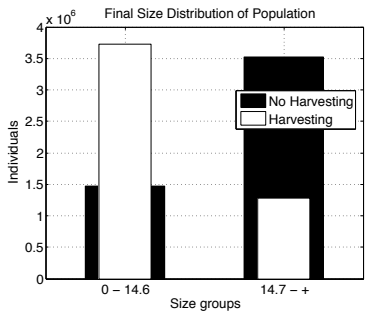

(c) Final distribution of population by size group.

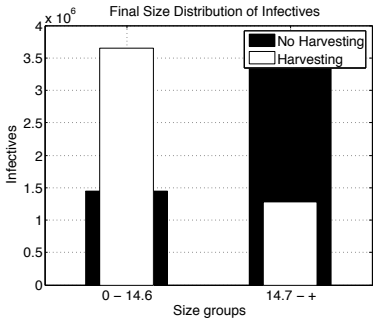

(d) Final distribution of infectives by size group.

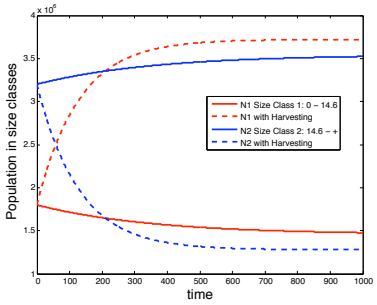

(e) Population dynamics for the two size groups. Population in this case is constant.

Figure 15: SI Constant Population, 2 Size Classes

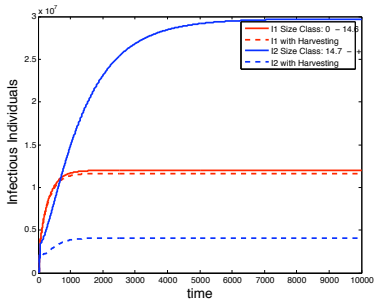

(a) Infectious individuals over time.

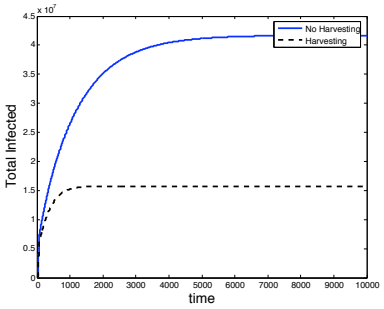

(b) Total infected over time.

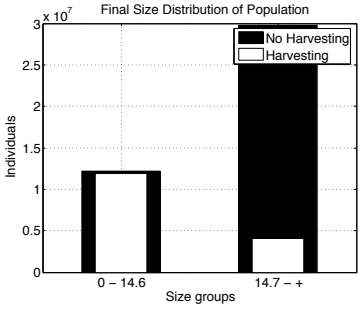

(c) Final distribution of population by size group.

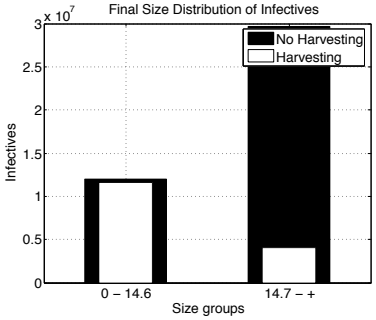

(d) Final distribution of infectives by size group.

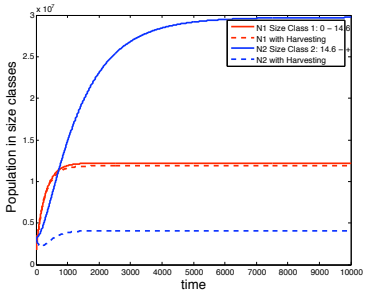

(e) Population dynamics for the two size groups. Population in this case is constant.

Figure 16: SI Constant Input, 2 Size Classes

4.4.2. Simulations with Higher Harvesting of Smaller Fish

In the SI model it is impossible to drive the number of infected individuals to zero, but we want to observe what is the effect of implementing a different harvesting strategy. In the first case with constant population we observe that the number of infections are reduced in both size classes; 17a, 17b. Harvesting produces a small reduction in the second size group and increment in the first size group 17c.

In the second case, the harvesting reduces considerably the population 18d and same behavior is observed in the infected population 18a, 18b. This is not considered a good alternative policy because it almost exterminate the population, but we observe that this reduced the population much more than the previous case because here the feeding is a lot less than the harvesting in the first class and if that class is reduced obviously the second class will get reduced too.

In the simulations for the SI model with higher harvesting rate of larger fish produces a small reduction in the infections. In the case of constant population it is just an effect of the change in the population proportions. In the case of non-constant population the infections get reduced because the harvesting reduces the population significantly. In the case of higher harvesting for smaller fish and almost no harvesting of large fish, the endemic infection lev-

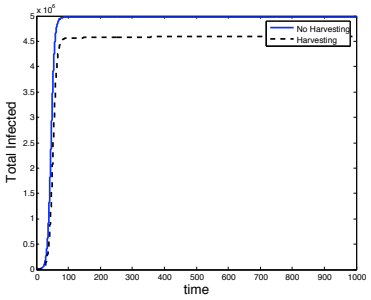

(a) Total infected over time.

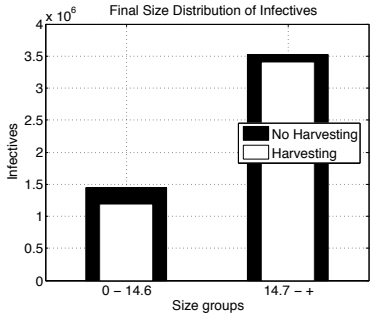

(b) Final distribution of infectives by size group.

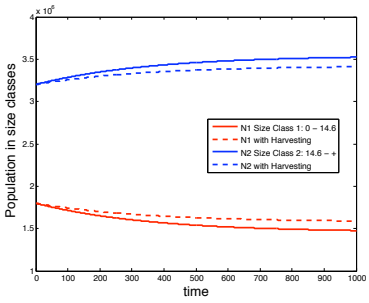

(c) Population dynamics for the two size groups. Population in this case is constant.

Figure 17: SI Constant Population, 2 Size Classes

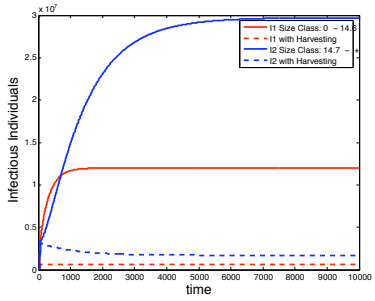

(a) Infectious individuals over time.

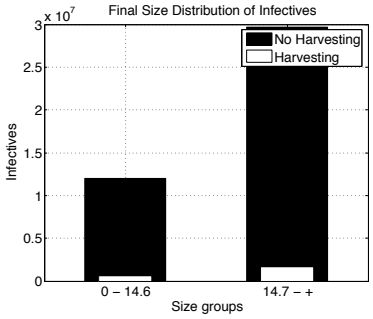

(b) Final distribution of infectives by size group.

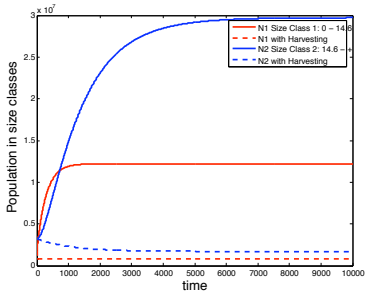

(c) Population dynamics for the two size groups. Population in this case is constant.

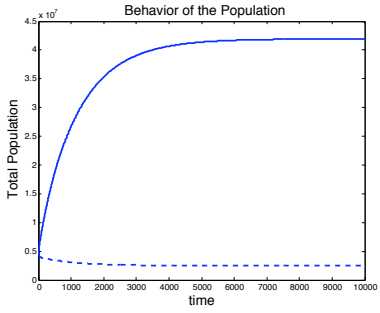

(d) Population dynamics.

Figure 18: SI Constant Input, 2 Size Classes

els get largely reduced because population is also greatly affected. In this case, changing the harvesting strategy does not control completely the disease since there is no recovery. Therefore, it is not recommended to use the strategy of harvesting larger amount of small fish during an outbreak of a disease from which fish do not recover because it does not help control the disease completely and it causes a big decrease in the population number.

4.4.3. SI Case $n = 3$: Simulations with Higher Harvesting of Larger Fish

Again, in the first case the population is constant and the same number of harvested elements are introduced in the population into the first size class. Results are consistent with the simulations for two sizes. The harvesting reduced the bigger size class and increases the first one 19a, 19d. And the same effect is observed in the population dynamics 19c, 19e. Also, there is no great reduction of infection 19b. In this second case, the results are also consistent with the results in the two classes. The harvesting reduced the population growth 20c, 20e, 20f. And this effect in the population is reflected in the infected population 20a, 20b, 20d.

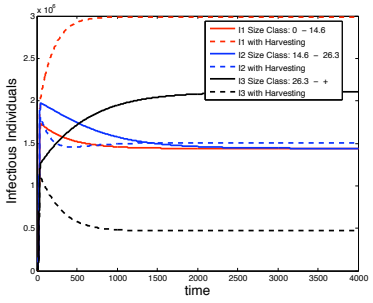

(a) Infectious individuals over time.

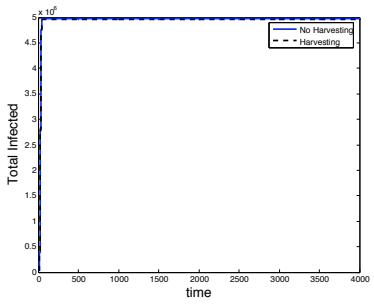

(b) Total infected over time.

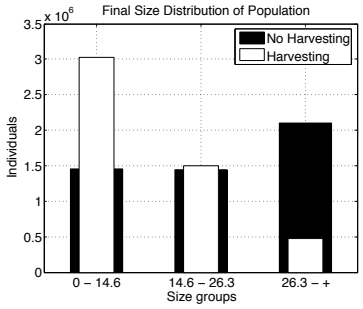

(c) Final distribution of population by size group.

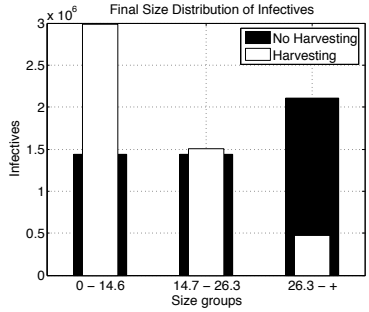

(d) Final distribution of infectives by size group.

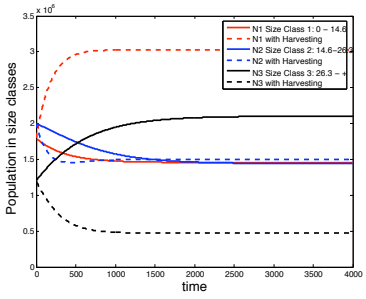

(e) Population dynamics for the two size groups. Population in this case is constant.

Figure 19: SI Constant Population, 3 Size Classes

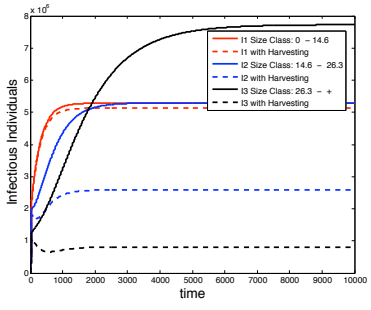

(a) Infectious individuals over time.

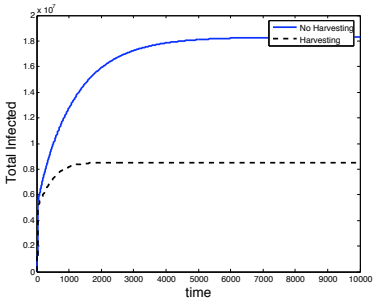

(b) Total infected over time.

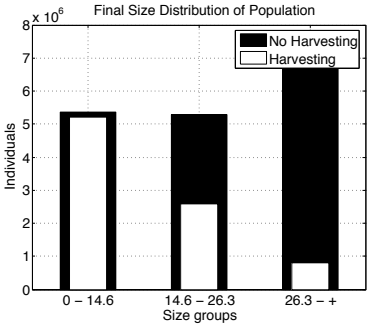

(c) Final distribution of population by size group.

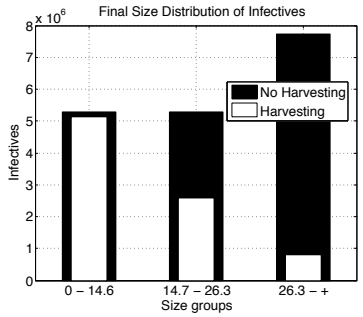

(d) Final distribution of infectives by size group.

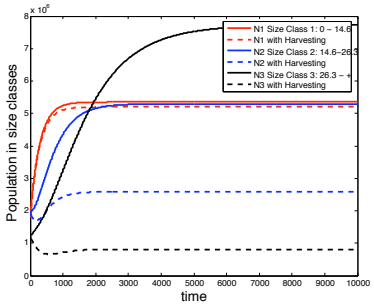

(e) Population dynamics for the two size groups. Population in this case is constant.

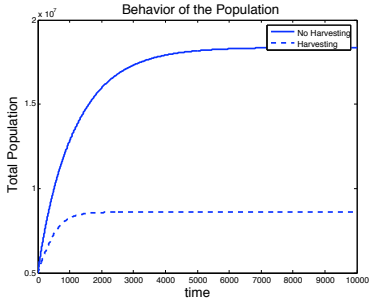

(f) Population dynamics.

Figure 20: SI Constant Input, 3 Size Classes

4.4.4. Simulations with Higher Harvesting of Smaller Fish and Decreasing Rates with Size

In this strategy of harvesting more harvesting occurs in the first size class which is the one with higher transmission rate and then the harvesting is decreasing with size. As in the two classes, the total number of infections is reduced 21a because the number of infections increases in the first size class and decreases in the other two 21b. Which is a consequence of the same behavior in the population by size dynamics over time 21c. In the second case, we have constant feeding of the population and the harvesting is higher in the first size class. Again the harvesting reduced the population and therefore the number of infections22a, 22b, 22c.

Similar to the case of two size classes, when we consider three size classes we observe that with higher harvesting of larger fish the infections get reduced in a very small number given the change in behavior in the whole population. In the case of constant population the proportions in the population switch to higher proportion of small fish. In the case of non-constant population, the harvesting produces a large decrease in the infections because the population is also decreased in a large number. With higher harvesting of smaller fish the infections are reduced even more, but the effect in the whole population is too

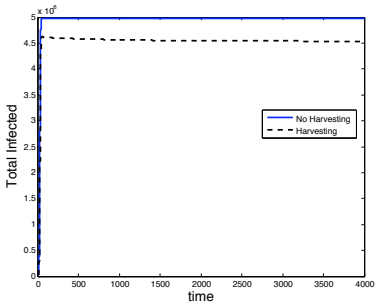

(a) Total infected over time.

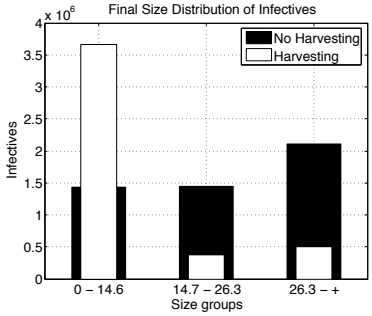

(b) Final distribution of infectives by size group.

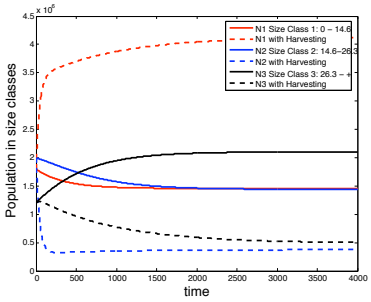

(c) Population dynamics for the two size groups. Population in this case is constant.

Figure 21: SI Constant Population, 3 Size Classes

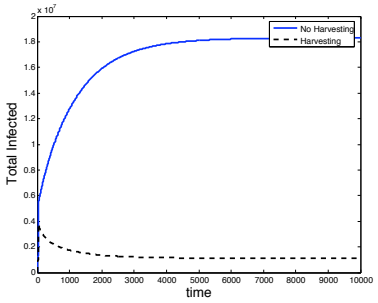

(a) Total infected over time.

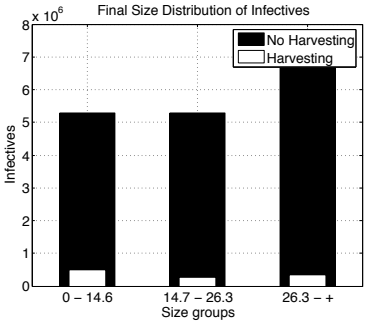

(b) Final distribution of infectives by size group.

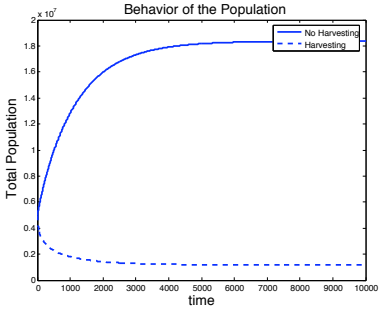

(c) Population dynamics.

Figure 22: SI Constant Input, 3 Size Classes

drastic and since it does not eliminates the infections it is a policy that will have to be kept infinitely to keep those infection levels. As we know this is not a policy that can be kept for indefinite time, therefore harvesting more small fish in an outbreak is not a good strategy in the case of an SI disease.

4.5. Conclusions

In this chapter the size-structured equation in Model (2.1) is discretized by size using the first principles of this model. We follow the approach used in Hethcote [13]. In Section 4.1, a similar approach is implemented to the SIR model (3.1)-(3.6) in populations where there are no demographic changes. This approach will give a $3n$ ordinary differential equations model (4.9)-(4.11), for n number of size groups, that has the same principles as the PDE model. Section 4.2 presents the specific case of two size classes. For this case we were able to calculate the disease free steady state and the basic reproductive number R_0. We explain the terms in the expression for R_0 using the different interactions of the two size groups. This expression takes into account the interactions between members of the same size and between different sizes as expected.Using Routh-Hurwitz criterion we were able to find conditions for local stability of the disease free equilibrium and the endemic equilibrium.

Some simulations were performed with different harvesting strategies or policies with the purpose of comparing those. For the harvesting strategies studied we considered the following cases: constant population, were the same number of harvested fish were reintroduced into the population in the susceptible class, constant feeding, were the number of births was constant and in the susceptible stage, and finally the case of proportional feeding were the number of births was proportional to the population. First, we started by simulating higher harvesting on large fish populations and relatively small harvesting for small fish as it is usually done in fishing. For the case of constant population, harvesting increases the number of infectives due to the way the population is fed to keep it constant. For constant feeding, harvesting affected in a positive way the disease outcome by reducing the number of total infections in the population but in a very small number. In feeding proportional to the population, although the number of infected individuals will be smaller with harvesting, the population will be smaller too and hence the proportion of infected individuals will be higher.

Same three cases were considered for higher harvesting rate of smaller fish and very small harvesting rate for bigger fish. In all three cases the new harvesting policy eliminated the number of infections in the population in a very short time. This makes us conclude that in the case of an outbreak it will be convenient to

harvest smaller fish in a high proportion to control the disease. But this strategy should not be implemented for longer after the disease is eradicated from the population since it reduced the population in the cases of constant feeding and proportional feeding. For the SIR with three classes we also performed simulations and the results were similar to the ones for the two size classes.

In Section 4.4, we implemented Hethcote's approach [13] to the SI model (**??**)-(**??**). For the SI $2n$ ordinary differential equations model we performed simulations using the same two harvesting strategies as for the SIR. Results were similar for two size classes and three size classes. When we considered higher harvesting rates in larger fish, as in the SIR, the harvesting reduced in a very small amount the number of infections. With higher harvesting rate in smaller fish the infections got reduced significantly but the disease remained endemic in a lower value. In the cases of constant feeding and proportional feeding the new strategy reduced the population drastically. This policy should not be implemented at the time of an outbreak if the disease does not have recovery because it does not eliminates the disease from the population and it affects adversely the population. The situation was quantitatively different but qualitatively the same for the SI model.

CHAPTER 5

OPTIMAL CONTROL PROBLEM

5.1. Constant Harvesting Effort, $n = 2$ Two Size Classes

In the previous sections we considered harvesting rates that were dependent on size and independent of time. Harvesting rates were constant in each size group. In this section we use time dependent harvesting rates that are also size dependent, since each size group has a different time dependent function for the harvesting. This method allows studying policies that change over time and will support the results in the previous sections where we concluded that changing harvesting strategy changed the outcome of the outbreak and by implementing it for a small time will control the disease completely.

This approach is only implemented for SIR, since new harvesting strategies do not control disease in the SI model.

When we consider harvesting the expression for R_0 is

$$R_0 = \frac{1}{2}\left[\frac{\beta b_1^2}{\gamma_1 + g_1 c_1 + \theta_1 + H_1} + \frac{\beta b_2^2}{\gamma_2 + \theta_2 + H_2}\right. \tag{5.1}$$

$$\left. + \sqrt{\left(\frac{\beta b_1^2}{\gamma_1 + g_1 c_1 + \theta_1 + H_1} + \frac{\beta b_2^2}{\gamma_2 + \theta_2 + H_2}\right)^2 + \frac{4\beta b_1 b_2 \theta_2}{(\gamma_2 + \theta_2 + H_2)(\gamma_1 + g_1 c_1 + \theta_1 + H_1)}}\right].$$

Which is smaller than (4.22). In order to have an outbreak (4.22) has to be greater

than one, therefore there is a critical harvesting rate at which the dynamics of the system change from outbreak to no outbreak. The motivation is to find this critical harvesting that can control the disease.

The next step for harvesting is running simulations considering time dependent harvesting rates.

5.2. Optimal Time-Dependent Harvesting

The model with size-specific controls is described by the following system of differential equations:

$$\begin{aligned}
\frac{dS_1}{dt} &= \rho - \left(\frac{\beta b_1^2}{N_1} I_1 + \frac{\beta b_1 b_2}{N_2} I_2 + g_1 c_1 + \theta_1 + H_1(t)\right) S_1, \\
\frac{dS_2}{dt} &= g_1 c_1 S_1 - \left(\frac{\beta b_2 b_1}{N_1} I_1 + \frac{\beta b_2^2}{N_2} I_2 + \theta_2 + H_2(t)\right) S_2, \\
\frac{dI_1}{dt} &= \frac{\beta b_1^2}{N_1} I_1 S_1 + \frac{\beta b_1 b_2}{N_2} I_2 S_1 - (\gamma_1 + \theta_1 + g_1 c_1 + H_1(t)) I_1, \qquad (5.2) \\
\frac{dI_2}{dt} &= g_1 c_1 I_1 + \frac{\beta b_2 b_1}{N_1} I_1 S_2 + \frac{\beta b_2^2}{N_2} I_2 S_2 - (\gamma_2 + \theta_2 + H_2(t)) I_2, \\
\frac{dR_1}{dt} &= \gamma_1 I_1 - (\theta_1 + g_1 c_1 + H_1(t)) R_1, \\
\frac{dR_2}{dt} &= g_1 c_1 R_1 + \gamma_2 I_2 - (\theta_2 + H_2(t)) R_2.
\end{aligned}$$

where the time dependent harvesting rates $H_1(t)$ and $H_2(t)$ serve as the control measures. The control functions $H_1(t)$ and $H_2(t)$ have values between zero and one, where one represents full effort and zero no effort implemented to control.

The goal is to minimize the number of infectious individuals $(I_1(t), I_2(t))$ over a finite time interval from zero to t_f at a minimal cost of harvesting efforts during a fish disease outbreak. The objective functional J is

$$J(H_1(t), H_2(t)) = \int_0^{t_f} (I_1(t) + I_2(t) + \frac{B_1}{2} H_1^2(t) + \frac{B_2}{2} H_2^2(t))dt \tag{5.3}$$

The optimal control problem is to find optimal solutions $(I_1^*(t), I_2^*(t), H_1^*(t), H_2^*(t))$ such that Goal:

$$J(H_1^*, H_2^*) = min_{\Omega} J(H_1, H_2) \tag{5.4}$$

for $i = 1, 2$, a_i and $b_i \in [0, 1]$.

$$\Omega = \{(H_1(t), H_2(t)) \in L^1(0, t_f)^2 || a_i \leq H_i(t) \leq b_i, t \in [0, t_f])\} \tag{5.5}$$

subject to the state equations given by the model (5.2). Given the criterion (5.3) and the regularity of the system of equations (5.2), the existence of optimal controls is guaranteed by standard results in control theory by Fleming and Rishel [11]. The necessary conditions of optimal solutions are derived from

Pontryagin's Maximum Principle [24]. The hamiltonian H is given by:

$$\begin{aligned} H &= I_1 + I_2 + \frac{B_1}{2}H_1^2 + \frac{B_2}{2}H_2^2 \\ &+\lambda_1\left(\rho - \left(\frac{\beta b_1^2}{N_1}I_1 + \frac{\beta b_1 b_2}{N_2}I_2 + g_1c_1 + \theta_1 + H_1(t)\right)S_1\right) \\ &+\lambda_2\left(g_1c_1S_1 - \left(\frac{\beta b_2 b_1}{N_1}I_1 + \frac{\beta b_2^2}{N_2}I_2 + \theta_2 + H_2(t)\right)S_2\right) \\ &+\lambda_3\left(\frac{\beta b_1^2}{N_1}I_1S_1 + \frac{\beta b_1 b_2}{N_2}I_2S_1 - (\gamma_1 + \theta_1 + g_1c_1 + H_1(t))I_1\right) \\ &+\lambda_4\left(g_1c_1I_1 + \frac{\beta b_2 b_1}{N_1}I_1S_2 + \frac{\beta b_2^2}{N_2}I_2S_2 - (\gamma_2 + \theta_2 + H_2(t))I_2\right) \\ &+\lambda_5\left(\gamma_1I_1 - (\theta_1 + g_1c_1 + H_1(t))R_1\right) + \lambda_6\left(g_2c_1R_1 + \gamma_2I_2 - (\theta_2 + H_2(t))R_2\right) \end{aligned} \tag{5.6}$$

The principle of Pontryagin coverts the system (5.2) into the problem of minimizing the hamiltonian H. From Pontryagin's Maximum Principle [24] we obtain the following theorem.

Theorem 5.1 *There exist optimal controls $H_1^*(t), H_2^*(t)$ and corresponding solutions $I_1^*(t), I_2^*(t)$ that minimize $J(H_1, H_2)$ over Ω. In order for the above state-*

ment to be true, it is necessary that there exist continuous functions λ_i such that:

$$\begin{aligned}
\frac{d\lambda_1}{dt} &= \lambda_1\left(\frac{\beta b_1^2}{N_1}I_1+\frac{\beta b_1 b_2}{N_2}I_2+g_1c_1+\theta_1+H_1(t)\right)-\lambda_2 g_1c_1 \\
&\quad -\lambda_3\left(\frac{\beta b_1^2}{N_1}I_1+\frac{\beta b_1 b_2}{N_2}I_2\right) \\
\frac{d\lambda_2}{dt} &= \lambda_2\left(\frac{\beta b_1 b_2}{N_1}I_1+\frac{\beta b_2^2}{N_2}I_2+\theta_2+H_2(t)\right)-\lambda_4\left(\frac{\beta b_1 b_2}{N_1}I_1+\frac{\beta b_2^2}{N_2}I_2\right) \\
\frac{d\lambda_3}{dt} &= -1+\lambda_1\frac{\beta b_1^2}{N_1}S_1+\lambda_2\frac{\beta b_1 b_2}{N_1}S_2-\lambda_3\left(\frac{\beta b_1^2}{N_1}S_1-(\gamma_1+\theta_1+g_1c_1+H_1(t))\right) \\
&\quad -\lambda_4\left(g_1c_1+\frac{\beta b_1 b_2}{N_1}S_2\right)-\lambda_5\gamma_1 \qquad (5.7) \\
\frac{d\lambda_4}{dt} &= -1+\lambda_1\frac{\beta b_1 b_2}{N_2}S_1+\lambda_2\frac{\beta b_2^2}{N_2}S_2-\lambda_3\frac{\beta b_1 b_2}{N_2}S_1 \\
&\quad -\lambda_4\left(\frac{\beta b_2^2}{N_2}S_2-(\gamma_2+\theta_2+H_2(t))\right)-\lambda_6\gamma_2 \\
\frac{d\lambda_5}{dt} &= \lambda_5(\theta_1+g_1c_1+H_1(t))-\lambda_6 g_1c_1 \\
\frac{d\lambda_6}{dt} &= \lambda_6(\theta_2+H_2(t))
\end{aligned}$$

subject to the transversality conditions,

$$\lambda_i(t_f)=0 \qquad (5.8)$$

for all $i=1,2,3,4,5,6$.

Proof: The existence of optimal controls follows from Corollary 4.1 of Fleming and Rishel [11] since the integrand of J is a convex function of $H_1(t), H_2(t)$ and the state system satisfies the Lipschitz property with respect to the state variables. The following can be derived from the Pontryagin's maximum principle

(Pontryagin et al. [24]):

$$\frac{d\lambda_1}{dt} = -\frac{\partial H}{\partial S_1}, \qquad \frac{d\lambda_2}{dt} = -\frac{\partial H}{\partial S_2}, \qquad \frac{d\lambda_3}{dt} = -\frac{\partial H}{\partial I_1},$$
$$\frac{d\lambda_4}{dt} = -\frac{\partial H}{\partial I_2}, \qquad \frac{d\lambda_5}{dt} = -\frac{\partial H}{\partial R_1}, \qquad \frac{d\lambda_6}{dt} = -\frac{\partial H}{\partial R_2},$$

with $\lambda_i(T) = 0$ for $i = 1, 2, ..., 6$ and evaluated at the optimal controls and corresponding states, which results in the adjoint system (5.7). The Hamiltonian H is minimized with respect to the controls, so we differentiate H with respect to H_i on the set Ω, respectively, giving the following optimality conditions:

$$\frac{\partial H}{\partial H_1} = 0, \frac{\partial H}{\partial H_2} = 0 \tag{5.9}$$

and solving for H_1^* and H_2^* with the constraints given by (5.5), the following characterization holds

$$H_1^*(t) = min(max(a_1, \frac{1}{B_1}(\lambda_1 S_1^* + \lambda_3 I_1^* + \lambda_5 R_1^*)), b_1), \tag{5.10}$$
$$H_2^*(t) = min(max(a_2, \frac{1}{B_2}(\lambda_2 S_2^* + \lambda_4 I_2^* + \lambda_6 R_2^*)), b_2). \tag{5.11}$$

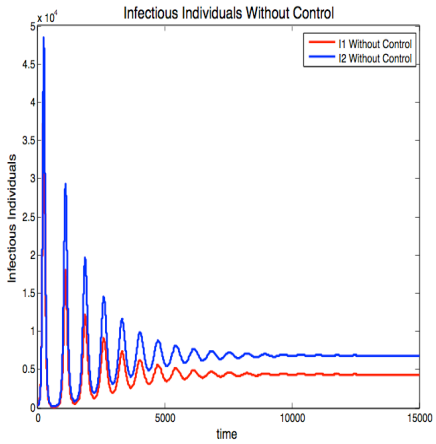

Figure 23: Infectious Individuals Without Control

If population is preserved constant by replacing the harvested individuals in the population by disease free individuals of size one, then we get the following results:

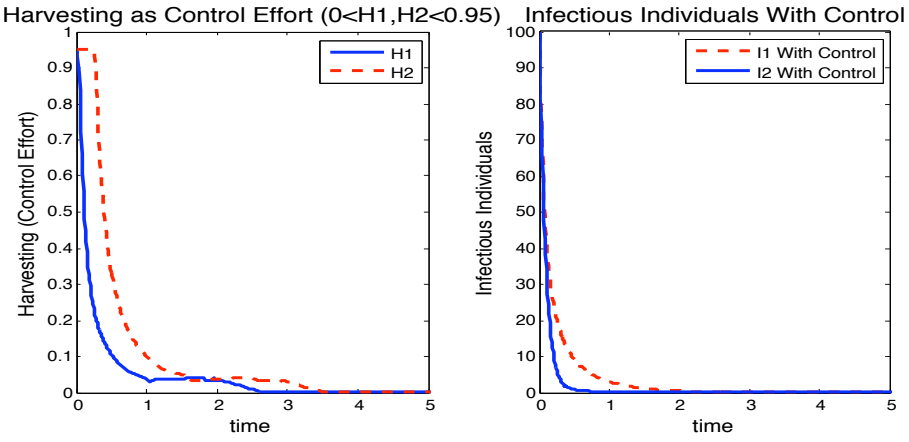

Figure 24: High levels of harvesting for both Size Groups. Disease dies out very quickly with no increment in the infectious individuals.

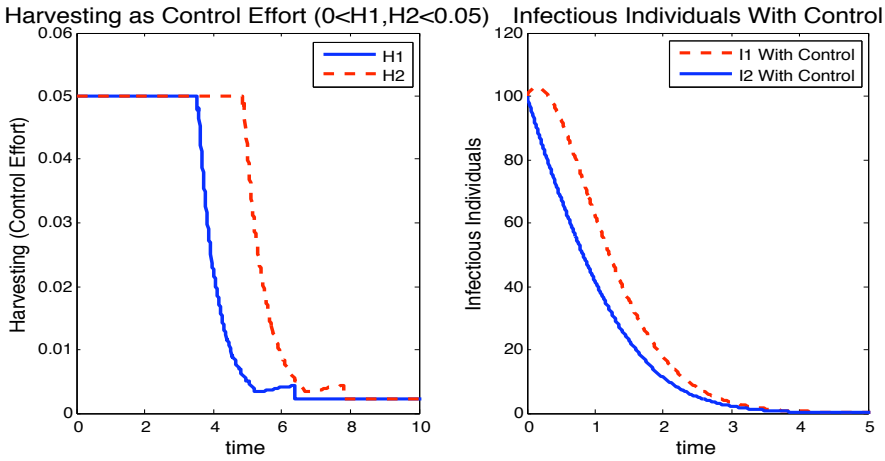

Figure 25: Low levels of harvesting for both Size Groups. Disease dies out very quickly but the infectious individuals in group 1 increase a little bit before they start getting reduced.

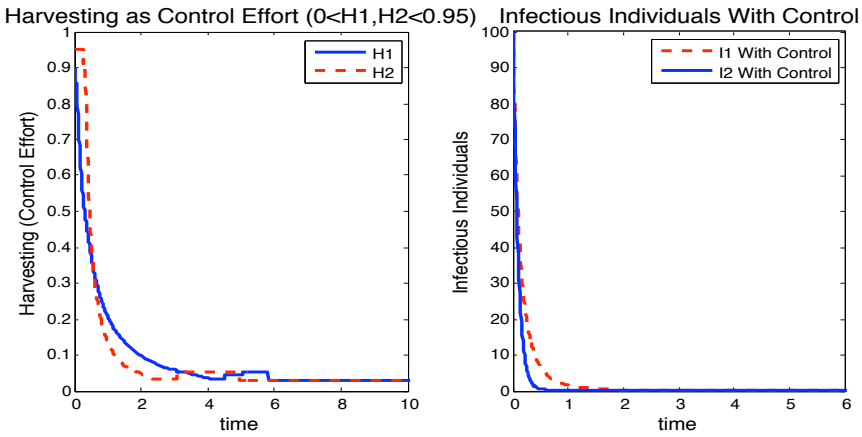

Figure 26: High levels of harvesting for both Size Groups. Disease dies out very quickly with no increment in the infectious individuals.

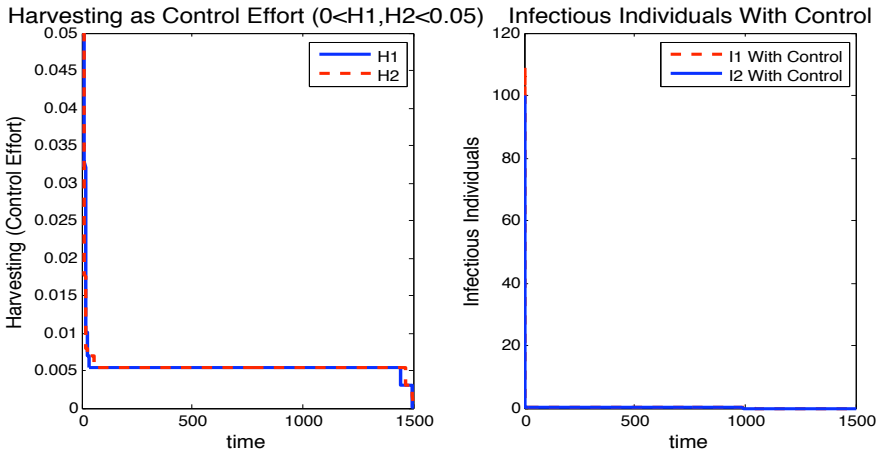

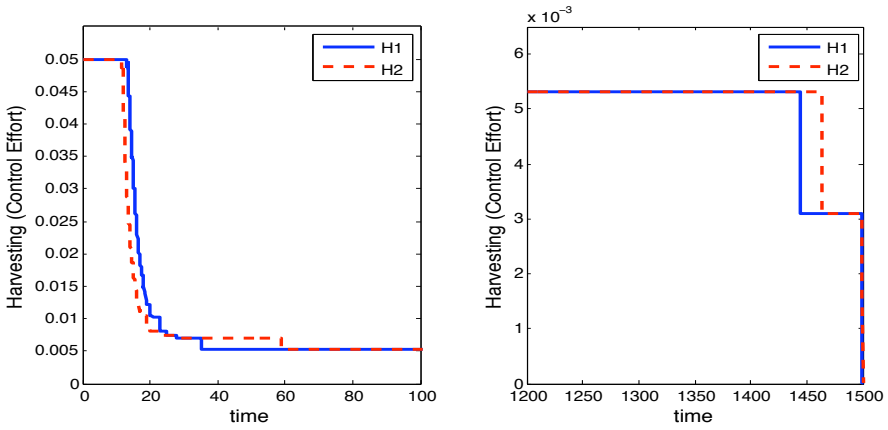

Figure 27: Low levels of harvesting for both Size Groups. Disease dies out very quickly but the infectious individuals in group 1 increase a little bit before they start getting reduced.

These simulations support the results in the previous sections, if the harvesting rates are not high enough then the infectious are not reduced to zero. If the harvesting rates are very high the control code suggests to harvest to the highest possible value on all size groups since this will reduce faster the infected. But at the same time, it is not desired to harvest all members of the population because that will be like replacing the population.

If low levels of harvesting are implemented in both size groups the disease cannot be controlled, if we harvest a lot of fish in both size groups because obviously we are replacing most of the population by uninfected fish. As in 4.1, if smaller fish have higher harvesting rates even when larger fish have lower harvesting rates the disease is control in a short time and then there is no need to continue harvesting so many small fish.

5.3. Conclusions

In this chapter, we analyzed the optimal control problem implemented on SIR model (5.2). Here we used Pontryagin's Maximum Principle [24] to derive the necessary conditions for optimal solutions that minimize the number of infected $(I_1(t), I_2(t))$ at minimal cost of harvesting, which is given by B_1 and B_2. Simulations support the results of the ODE SIR model in Chapter 5. If harvest-

ing rates are not high enough, specially for smaller fish, the outbreak cannot be controlled and disease remains endemic in the population. If the harvesting rate is high for smaller fish, then the disease is controlled faster. When high harvesting rates are implemented, the disease goes to extinction fast and there is no need to continue harvesting massively.

CHAPTER 6

CONCLUSIONS

In this study we analyzed the effect of structuring the population by size explicitly via a per-capita growth function $g(m)$. Results on harvesting affects on a size structure populations at demographic ($q^* = 0$) equilibrium or changing ($q \neq 0$) were revisited. The main contribution of this dissertation is through the introduction of a SIR epidemic model with size structure; a model analyzed partially at demographic equilibrium ($q^* = 0$).

A $3n$-epidemic SIR ODE model using the approach introduced by Hethcote [13] in the context of age-structure populations, was introduced. A partial analysis of the case $n = 2$ was carried out. Simulations that explored the role of harvesting were carried out in the cases $n = 2$ and $n = 3$.

Since often individuals in the wild do not recover we proceeded to simulate the $n = 2$ and $n = 3$ cases for an *SI*-disease. We found (as expected) quantitative differences but not qualitative. In other words, *SIR* and *SI* models has similar dynamics.

The different simulations performed showed that, under the assumed parameters, it is good to change harvesting policies that do not provide great benefits for the fishermen like fishing smaller fish. These changes in policy make a huge difference in the outcome of the disease and in many cases controlled the dis-

ease completely in a small frame of time. If this effect of the harvesting policy changes are obtained so fast, it could be a good strategy that can be put into action until the disease is controlled. Then usual harvesting policies can continue and fishermen can continue getting the benefits desired.

In chapter 5, control theory was implemented with the purpose of getting optimal harvesting policies to reduce a disease in an SIR model. Some of the results in this chapter support the ones in the previous chapters. Very small harvesting rates in all size groups do not support the control of the disease and we can observe that the disease remains endemic. Harvesting rates should be high enough to take off enough infected elements and reduce infection in the population. The bad side of our control-function approach is that in our approach we did not focus on the measure that considered optimal biomass. Hence, controlling the disease may drive the population to extinction. In other words, improvements in the control formulation are required. Our results offer only a preliminary perspective on their role in size-dependent harvesting.

REFERENCES

[1] Aranguren R., Tafalla C., Novoa B. and Figueras A. (2002) Experimental transmission of encephalopathy and retinopathy induced by nodavirus to sea bream, Sparus aurata L., using different infection models. Journal of Fish Diseases 25, 317-324.

[2] Becker J.A., Speare D.J., and Dohoo I.R. (2005) Influence of feeding ratio and size on susceptibility to microsporidial gill disease caused by Loma salmonae in rainbow trout, Oncorhynchus mykiss (Walbaum). Journal of Fish Diseases 28, 173-180.

[3] Bowser P.R., Wooster G.A. and Earnest-Koons K. (1997) Effects of fish age and challenge routes in experimental transmission of walleye dermal sarcoma in walleyes by cell-free tumor filtrates. Journal of Aquatic Animal Health 9, 274-278.

[4] Brauer, F., Castillo-Chavez, C. (2001) Mathematical Models in Population Biology and Epidemiology. Springer-Verlag New York, Inc.

[5] Busenberg, S., Castillo-Chavez, C. (1991) A general solution of the problem of mixing of sub-populations and its application to risk- and age-structured models for the spread of AIDS, IMA Journal of Mathematical Applications to Medical Biology 8, 1-29.

[6] Busenberg S., Cooke K., Iannelli M. (1988) Endemic Thresholds and Stability in a Class of Age-Structured Epidemics, SIAM Journal on Applied Mathematics 48(6), 1379-1395.

[7] Busenberg, S., Iannelli, M., Thieme, H., (1991) Global behavior of an age-structured epidemic model. SIAM Journal of Mathematical Analysis 22, 1065-1080

[8] Castillo-Chavez, C. (1987) Linear Character-Dependent Models with Constant Time Delay in Population Dynamics. Math! Modeling, 9(11), 821-836 .

[9] Castillo-Chavez, C., Hethcote, H.W. , Andreasen, V. , Levin, S.A. and Liu, W.M. (1989) Epidemiological models with age structure, proportionate mixing, and cross immunity. J. Math. Biol. 27: 233-258.

[10] Fenichel, E. P., Tsao, J. I. and Jones, M. L. (2009) Modeling fish health to inform research and management: Renibacterium salmoninarum dynamics in Lake Michigan. Ecological Applications 19(3): 747-760.

[11] Fleming, W.H., Rishel, R.W. (1975) Deterministic and Stochastic Optimal Control. New York: Springer.

[12] Gisser, M., and Sanchez, D. A. (1980) Competition Versus Optimal Control in Groundwater Pumping. Water Resources Research, 16(4), 638-642.

[13] Hethcote, H.W. (1997) An Age-Structured Model for Pertussis Transmission.Mathematical Biosciences 145, 89-136 .

[14] Hoppensteadt, F. (1975) Mathematical Theories of Populations: Demographics, Genetics and Epidemics.

[15] Huang, W., Cooke, K., Castillo-Chavez, C., (1992) Stability and bifurcation for a multiple-group model for the dynamics of HIV/AIDS transmission, SIAM Journal of Applied Mathematics 52, 835-854.

[16] Kato, N. (2008) Optimal Harvesting for nonlinear size-structured population dynamics. J. Math. Anal. Appl. 342, 1388 - 1398.

[17] Kato, N., Oharu, S., and Shitaoka, K. (2007) Size-structured plat population models and harvesting problems. Journal of Computational and Applied Mathematics 204, 114 - 123.

[18] Langlais M., Milner F.A. (1994) Separable Solutions of an Age-Dependent Population Model with Age Dominance and Their Stablity. Mathematical Biosciences 119: 115-125.

[19] Lasater J.E. and Haw F. (1964) The Relationship of Age to Length in Puget Sound Resident Chinook Salmon, 2(3), 44-50.

[20] LaPatra S.E., Groberg W.J., Rohovec J.S. and Fryer J.L. (1990) Size-related susceptibility of salmonids to two strains of infectious hematopoietic necrosis virus. Transactions of the American Fisheries Society 199, 25-30.

[21] Levin, S.A., Hallam, T.G., and Gross, L.J. (1989) Applied Mathematical Ecology. Biomathematics Texts, Springer-Verlag .

[22] Nisbet, R.M., Gurney, W.S.C. (1982) Modelling Fluctuating Populations.John Wiley & Sons Ltd.

[23] Perelberg A., Smirnov M., Hutoran M., Diamant A., Bejerano Y. and Kolter M. (2003) Epidemiological description of a new viral disease afflicting cultured Cyprinus carpio in Israel. Israeli Journal of Aquaculture 55, 5-12.

[24] Pontryagin, L. S., Boltyanskii, V. G., Gamkrelidze, R. V., Mishchenko, E. F. (1962). The mathematical theory of optimal processes. New Jersey: Wiley.

[25] Sanchez, D.A. (1978) Linear Age-Dependent Population Growth with Harvesting. Bulletin of Mathematical Biology, 40(3), 377-385.

[26] Sanchez, D.A. (1980) Linear Age-Dependent Population Growth with Seasonal Harvesting. Journal of Mathematical Biology, 9(4), 361-368.

[27] Sinko, J. W., Streifer, W. (1967) A New Model For Age-Size Structure of a Population. Ecology, 48(6), 910-918.

APPENDIX A

SOLUTION OF STABLE SIZE DISTRIBUTIONS

$$\begin{aligned}
\frac{\partial S}{\partial t} + g(m)\frac{\partial S}{\partial m} &= -\lambda(t)b(m)S - \theta(m)S \\
\cancel{\rho} q \cancel{e^{qt}} s^* + \cancel{\rho} g(m) \cancel{e^{qt}} \frac{ds^*}{dm} &= -\cancel{\rho}\lambda^* b(m) \cancel{e^{qt}} s^* - \cancel{\rho}\theta(m) \cancel{e^{qt}} s^* \\
g(m)\frac{ds^*}{dm} &= -(q + \lambda^* b(m) + \theta(m))s^* \\
\frac{ds^*}{dm} &= -\frac{q + \lambda^* b(m) + \theta(m)}{g(m)} s^*
\end{aligned}$$

$$s^*(m) = s(m_0)\exp\left(-\int_{m_0}^{m} \frac{q + \lambda^* b(m') + \theta(m')}{g(m')} dm'\right) \tag{A.1}$$

$$\begin{aligned}
\frac{\partial I}{\partial t} + g(m)\frac{\partial I}{\partial m} &= \lambda(t)b(m)S(t,m) - (\gamma(m) + \theta(m))I(t,m) \\
\cancel{\rho} q \cancel{e^{qt}} i^* + g(m) \cancel{\rho} \cancel{e^{qt}} \frac{di^*}{dm} &= \lambda^* b(m) \cancel{\rho} \cancel{e^{qt}} s^* - (\gamma(m) + \theta(m)) \cancel{\rho} \cancel{e^{qt}} i^*
\end{aligned}$$

$$\begin{aligned}
g(m)\frac{di^*}{dm} + (q + \gamma(m) + \theta(m))i^* &= \lambda^* b(m) s^* \\
\frac{di^*}{dm} + \frac{q + \gamma(m) + \theta(m)}{g(m)} i^* &= \lambda^* \frac{b(m)}{g(m)} s^*
\end{aligned}$$

$$\frac{d}{dm}\left(\exp\left(\int_{m_0}^{m} \frac{q + \gamma(m') + \theta(m')}{g(m')} dm'\right) i^*\right) = \lambda^* s(m_0)\frac{b(m)}{g(m)} \exp\left(-\int_{m_0}^{m} \frac{\lambda^* b(\alpha) - \gamma(\alpha)}{g(\alpha)} d\alpha\right)$$

$$\exp\left(\int_{m_0}^{m} \frac{q + \gamma(m') + \theta(m')}{g(m')} dm'\right) i^* = \lambda^* s(m_0) \int_{m_0}^{m} \frac{b(m')}{g(m')} \exp\left(-\int_{m_0}^{m'} \frac{\lambda^* b(\alpha) - \gamma(\alpha)}{g(\alpha)} d\alpha\right) dm'$$

$$
\begin{aligned}
i^*(m) &= \lambda^* s(m_0) \exp\left(-\int_{m_0}^{m} \frac{q+\theta(m')}{g(m')} dm'\right) \int_{m_0}^{m} \frac{b(m')}{g(m')} \\
&\quad \exp\left(-\int_{m_0}^{m'} \frac{\lambda^* b(\alpha)}{g(\alpha)} d\alpha\right) \exp\left(-\int_{m'}^{m} \frac{\gamma(\alpha)}{g(\alpha)} d\alpha\right) dm'
\end{aligned}
$$

Since $\eta^*(m) = s^*(m) + i^*(m) + r^*(m)$, then $r^*(m) = \eta^*(m) - s^*(m) - i^*(m)$.

APPENDIX B

LINEARIZATION OF PERTURBATIONS TO STABLE SIZE DISTRIBUTION

Since $\zeta(t,m) = s^*(m) - s(t,m)$, the linearization about the steady state size distribution $p^* = (s^*, i^*, r^*, \lambda^*)$ of

$$\frac{ds}{dt} + g(m)\frac{ds}{dm} = -\lambda(t)b(m)s(t,m) - \theta(m)s(t,m)$$

is

$$\frac{d\zeta}{dt} + g(m)\frac{d\zeta}{dm} = a(m)\zeta(t,m) + b(m)\delta(t)$$

where

$$\begin{aligned} a(m) &= \frac{d}{ds}(-\lambda(t)b(m)s(t,m) - \theta(m)s(t,m))\Big|_{p^*} = -\lambda^* b(m) - \theta(m), \\ b(m) &= \frac{d}{d\lambda}(-\lambda(t)b(m)s(t,m) - \theta(m)s(t,m))\Big|_{p^*} = -b(m)s^*. \end{aligned}$$

Therefore,

$$\frac{d\zeta}{dt} + g(m)\frac{d\zeta}{dm} = -\lambda^* b(m)\zeta - \theta(m)\zeta - \delta(t)b(m)s^*. \tag{B.1}$$

Similarly for $i(t,m)$, where $\xi(t,m) = i^*(m) - i(t,m)$ the linearization about the steady state is

$$\frac{d\xi}{dt} + g(m)\frac{d\xi}{dm} = c(m)\zeta(t,m) + d(m)\xi(t,m) + e(m)\delta(t)$$

where

$$\begin{aligned} c(m) &= \frac{d}{ds}(\lambda(t)b(m)s-\gamma(m)i-\theta(m)i)\Big|_{p^*} = \lambda^* b(m), \\ d(m) &= \frac{d}{di}(\lambda(t)b(m)s-\gamma(m)i-\theta(m)i)\Big|_{p^*} = -\gamma(m)-\theta(m), \\ e(m) &= \frac{d}{d\lambda}(\lambda(t)b(m)s-\gamma(m)i-\theta(m)i)\Big|_{p^*} = b(m)s^*. \end{aligned}$$

Then, the linearized equation for $\xi(t,m)$ is

$$\frac{d\xi}{dt}+g(m)\frac{d\xi}{dm} = \lambda^* b(m)\zeta(t,m)-(\gamma(m)+\theta(m))\xi(t,m)+\delta(t)b(m)s^* \quad \text{(B.2)}$$

Finally,

$$\lambda(t)=\int_{m_0}^{\infty} b(m')i(t,m')dm'$$

$$\begin{aligned} \lambda^*+\delta(t) &= \int_{m_0}^{\infty} b(m')(i^*+\xi)dm' \\ \cancel{\lambda^*}+\delta(t) &= \cancel{\int_{m_0}^{\infty} b(m')i^* dm'}+\int_{m_0}^{\infty} b(m')\xi dm' \\ \delta(t) &= \int_{m_0}^{\infty} b(m')\xi(t,m')dm'. \end{aligned} \quad \text{(B.3)}$$

APPENDIX C

PERTURBATION

By substituting the perturbation of the form $\zeta(t,m) = e^{pt}\hat{\zeta}$ into equation 3.21,

$$\begin{aligned}
\frac{d\zeta}{dt} + g(m)\frac{d\zeta}{dm} &= -\lambda^* b(m)\zeta - \theta(m)\zeta - \delta(t)b(m)s^* \\
p\cancel{e^{pt}}\hat{\zeta} + g(m)\cancel{e^{pt}}\frac{d\hat{\zeta}}{dm} &= -\lambda^* b(m)\cancel{e^{pt}}\hat{\zeta} - \theta(m)\cancel{e^{pt}}\hat{\zeta} \\
&\quad -\cancel{e^{pt}}\hat{\delta}b(m)s^* \\
g(m)\frac{d\hat{\zeta}}{dm} + (p + \lambda^* b(m) + \theta(m))\hat{\zeta} &= -\hat{\delta}b(m)s^* \\
\frac{d\hat{\zeta}}{dm} + \frac{p + \lambda^* b(m) + \theta(m)}{g(m)}\hat{\zeta} &= -\hat{\delta}\frac{b(m)}{g(m)}s^*
\end{aligned}$$

$$\begin{aligned}
\frac{d\hat{\zeta}}{dm} + \frac{p + \lambda^* b(m) + \theta(m)}{g(m)}\hat{\zeta} &= -\hat{\delta}\frac{b(m)}{g(m)}s(m_0) \\
&\quad \exp\left(-\int_{m_0}^{m} \frac{q + \lambda^* b(m') + \theta(m')}{g(m')}dm'\right)
\end{aligned}$$

$$\begin{aligned}
\frac{d}{dm}\left(\exp\left(\int_{m_0}^{m} \frac{p + \lambda^* b(m') + \theta(m')}{g(m')}dm'\right)\hat{\zeta}\right) &= -\hat{\delta}\frac{b(m)}{g(m)} \\
&\quad \exp\left(-\int_{m_0}^{m} \frac{q}{g(m')}dm'\right)\exp\left(\int_{m_0}^{m} \frac{p}{g(m')}dm'\right)
\end{aligned}$$

$$\begin{aligned}
\exp\left(\int_{m_0}^{m} \frac{p + \lambda^* b(m') + \theta(m')}{g(m')}dm'\right)\hat{\zeta} &= -\hat{\delta}s(m_0)\int_{m_0}^{m} \frac{b(m')}{g(m')} \\
&\quad \exp\left(-\int_{m_0}^{m'} \frac{q}{g(\alpha}d\alpha\right)\exp\left(\int_{m_0}^{m'} \frac{p}{g(\alpha)}d\alpha\right)dm'
\end{aligned}$$

$$\begin{aligned}
\hat{\zeta}(m) &= -\hat{\delta}s(m_0)\exp\left(-\int_{m_0}^{m} \frac{\lambda^* b(m') + \theta(m')}{g(m')}dm'\right) \\
&\quad \int_{m_0}^{m} \frac{b(m')}{g(m')}\exp\left(-\int_{m_0}^{m'} \frac{q}{g(\alpha)}d\alpha\right)\exp\left(-\int_{m'}^{m} \frac{p}{g(\alpha)}d\alpha\right)dm' \qquad \text{(C.1)}
\end{aligned}$$

Similarly using $\xi(t,m) = e^{pt}\hat{\xi}$ into equation 3.24, we get

$$\begin{aligned}
\frac{d\xi}{dt} + g(m)\frac{d\xi}{dm} &= \lambda^* b(m)\zeta - (\gamma(m)+\theta(m))\xi + \delta(t)b(m)s^* \\
p\cancel{e^{pt}}\hat{\xi} + g(m)\cancel{e^{pt}}\frac{d\hat{\xi}}{dm} &= \lambda^* b(m)\cancel{e^{pt}}\hat{\xi} - (\gamma(m)+\theta(m))\cancel{e^{pt}}\hat{\xi} \\
&\quad + \hat{\delta}\cancel{e^{pt}}b(m)s^* \\
g(m)\frac{d\hat{\xi}}{dm} + (p+\gamma(m)+\theta(m))\hat{\xi} &= \lambda^* b(m)\hat{\zeta} + \hat{\delta}b(m)s^*
\end{aligned}$$

$$\begin{aligned}
&\frac{d\hat{\xi}}{dm} + \frac{p+\gamma(m)+\theta(m)}{g(m)}\hat{\xi} \\
&= -\lambda^*\frac{b(m)}{g(m)}\hat{\delta}s(m_0)\exp\left(-\int_{m_0}^{m}\frac{\lambda^* b(m')+\theta(m')}{g(m')}dm'\right)\int_{m_0}^{m}\frac{b(m')}{g(m')} \\
&\exp\left(-\int_{m_0}^{m'}\frac{q}{g(\alpha)}d\alpha\right)\exp\left(-\int_{m'}^{m}\frac{p}{g(\alpha)}d\alpha\right)dm' \\
&+\hat{\delta}\frac{b(m)}{g(m)}s(m_0)\exp\left(-\int_{m_0}^{m}\frac{q+\lambda^* b(m')+\theta(m')}{g(m')}dm'\right) \\
&\frac{d}{dm}\left(\exp\left(\int_{m_0}^{m}\frac{p+\gamma(m')+\theta(m')}{g(m')}dm'\right)\hat{\xi}\right) \\
&= \hat{\delta}s(m_0)\frac{b(m)}{g(m)}\exp\left(-\int_{m_0}^{m}\frac{\lambda^* b(m')}{g(m')}dm'\right)\exp\left(\int_{m_0}^{m}\frac{p+\gamma(m')}{g(m')}dm'\right) \\
&\left[\exp\left(-\int_{m_0}^{m}\frac{q}{g(m')}dm'\right) - \lambda^*\int_{m_0}^{m}\frac{b(m')}{g(m')}\right. \\
&\left.\exp\left(-\int_{m_0}^{m'}\frac{q}{g(\alpha)}d\alpha - \int_{m'}^{m}\frac{p}{g(\alpha)}d\alpha\right)dm'\right] \\
&\exp\left(\int_{m_0}^{m}\frac{p+\gamma(m')+\theta(m')}{g(m')}dm'\right)\hat{\xi} \\
&= \int_{m_0}^{m}\hat{\delta}s(m_0)\frac{b(m')}{g(m')}\exp\left(-\int_{m_0}^{m'}\frac{\lambda^* b(\alpha)}{g(\alpha)}d\alpha\right)\exp\left(\int_{m_0}^{m'}\frac{p+\gamma(\alpha)}{g(\alpha)}d\alpha\right) \\
&\left[\exp\left(-\int_{m_0}^{m'}\frac{q}{g(\alpha)}d\alpha\right) - \lambda^*\int_{m_0}^{m'}\frac{b(\alpha)}{g(\alpha)}\right. \\
&\left.\exp\left(-\int_{m_0}^{\alpha}\frac{q}{g(\omega)}d\omega - \int_{\alpha}^{m'}\frac{p}{g(\omega)}d\omega\right)d\alpha\right]dm'
\end{aligned}$$

$$
\begin{aligned}
\hat{\tilde{\xi}}(m) \;=\; & \hat{\delta} s(m_0) \exp\left(-\int_{m_0}^{m} \frac{\theta(m')}{g(m')} dm'\right) \int_{m_0}^{m} \frac{b(m')}{g(m')} \\
& \exp\left(-\int_{m_0}^{m'} \frac{\lambda^* b(\alpha)}{g(\alpha)} d\alpha\right) \exp\left(-\int_{m'}^{m} \frac{p+\gamma(\alpha)}{g(\alpha)} d\alpha\right) \\
& \left[\exp\left(-\int_{m_0}^{m'} \frac{q}{g(\alpha)} d\alpha\right) - \lambda^* \int_{m_0}^{m'} \frac{b(\alpha)}{g(\alpha)}\right. \\
& \left.\exp\left(-\int_{m_0}^{\alpha} \frac{q}{g(\omega)} d\omega - \int_{\alpha}^{m'} \frac{p}{g(\omega)} d\omega\right) d\alpha\right] dm' \qquad \text{(C.2)}
\end{aligned}
$$